Bioconjugate Chemistry

Article

pubs.acs.org/bc

Ligand-Directed Acid-Sensitive Amidophosphate 5-Trifluoromethyl-2′-Deoxyuridine Conjugate as a Potential Theranostic Agent

Tatyana S. Godovikova,*[,†,‡] Vladimir A. Lisitskiy,[†,‡] Natalya M. Antonova,[†,‡] Tatyana V. Popova,[†,‡] Olga D. Zakharova,[†] Alexey S. Chubarov,[†,‡] Igor V. Koptyug,[‡,§] Renad Z. Sagdeev,[§] Robert Kaptein,[‡,∥] Andrey E. Akulov,[⊥] Vassily I. Kaledin,[⊥] Valeriy P. Nikolin,[⊥] Sergei I. Baiborodin,[⊥] Ludmila S. Koroleva,[†,‡] and Vladimir N. Silnikov*[,†]

[†]Institute of Chemical Biology and Fundamental Medicine, SB RAS, 630090 Novosibirsk, Russia

[‡]Novosibirsk State University, 630090 Novosibirsk, Russia

[§]International Tomography Center, SB RAS, 630090 Novosibirsk, Russia

[∥]Bijvoet Center, University of Utrecht, 3584 CH Utrecht, The Netherlands

[⊥]Institute of Cytology and Genetics, SB RAS, 630090 Novosibirsk, Russia

Supporting Information

ABSTRACT: Herein, we report a novel strategy to engineer an acid-sensitive anticancer theranostic agent using a vector−drug ensemble. The ensemble was synthesized by directly conjugating the linoleic acid (LA)-modified branched polyethyleneimine with a chemotherapeutic drug trifluorothymidine. Linoleic acid residues were grafted onto 25 kDa polyethyleneimine (PEI) by treating PEI with linoleic acid chloroanhydride. 5-Trifluoromethyl-2′-deoxyuridine (trifluorothymidine, TFT) was introduced into LA-PEI conjugate by phosphorylating the conjugate with amidophosphate of trifluorothymidine 5′-monophosphate (pTFT), which had been activated by its conversion into the *N,N*-dimethylaminopyridine derivative. The extent of mononucleotide analog incorporation in the polymer was regulated by the ratio of pTFT to the polymer during the synthesis. Samples containing 20−70 TFT residues per PEI molecule were obtained. The cytotoxicity of PEI-LA-pTFT conjugates decreased with increasing nucleotide content, as examined using the MTT method. Due to the presence of fluorine atoms, TFT-based conjugates could be detected directly in the animals by ^{19}F magnetic resonance imaging. In addition, the presence of the amidophosphate group in PEI-LA-pTFT conjugates allowed their detection by *in vivo* ^{31}P NMR spectroscopy. Indeed, the ^{31}P NMR signal of a phosphoramide ($\delta \sim 12$ ppm) was observed in the mouse muscle tissue treated with PEI-LA-pTFT conjugate along with the signals from endogenous phosphorus-containing compounds. At the same time, the use of PEI-LA-pTFT conjugate for chemotherapeutic drug delivery is limited due to the low release of pTFT from the carrier. To enhance the release of the drug from the conjugate in the endosomes, PEI-LA polymer was coupled with urocanic acid (UA), which bears imidazole ring and thus can form an acid-labile P−N bond with pTFT. The PEI-LA-UA-pTFT conjugate containing 30 residues of UA and 40 residues of pTFT was tested against the murine Krebs-II ascites carcinoma, grown as an ascetic tumor. The intraperitoneal injection of the conjugates resulted in prolongation of the animals' life and to the complete disappearance of the tumor after three injections.

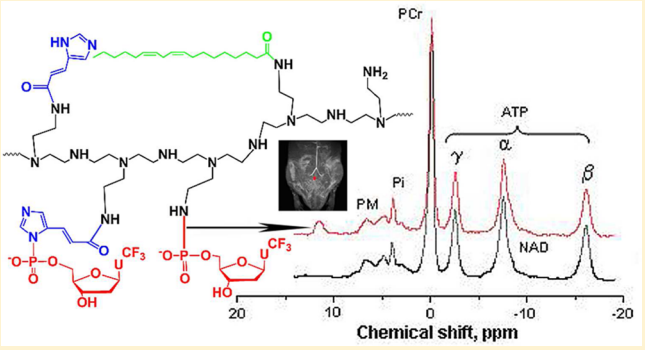

INTRODUCTION

A single agent that can be used to simultaneously diagnose and treat cancer, as well as to monitor a patient's response to the treatment, would be an ideal tool for health care providers.[1−5] Several approaches to combine targeted drug delivery with magnetic resonance imaging (MRI) have been reported.[4−7] MRI is a noninvasive technique that can provide detailed high-resolution tomographic information about a diseased tissue *in vivo* in real time. Hence, it has become a powerful diagnostic tool for the detection of the stages of primary and recurrent solid tumors, as well as for the assessment of suitable treatment regimens. Therefore, MRI is an attractive tool for the development of theranostic platforms for the post-treatment evaluation of solid tumors.

MRI studies are often conducted with the help of paramagnetic Gd^{III} complexes, which enhance the signal

Received: November 14, 2012
Revised: March 7, 2013
Published: March 22, 2013

   dx.doi.org/10.1021/bc3006072 | *Bioconjugate Chem.* 2013, 24, 780−795

intensity by reducing the longitudinal relaxation time (T_1) of water protons close to the Gd^{III} center.[7−9] As an example of theranostic agents, gadolinium-based perfluorocarbon nanoparticles have been used to detect, characterize, treat, and monitor angiogenesis in preclinical models of cancer and atherosclerosis.[10] Despite their preclinical success, some of the approved gadolinium-based MRI contrast agents have been implicated in the development of nephrogenic systemic fibrosis, which is a serious and unexpected side effect observed in some patients with renal disease or following liver transplant.[11] At the same time, ^{1}H contrast agents are not ideal tools for MRI, since the changes in image contrast in regions supposedly containing the labeled cells are often subtle and, therefore, difficult to interpret. In the body, mobile water creates large ^{1}H background signal, thus making it difficult to unambiguously identify the labeled cells *in vivo*, especially if the cell biodistribution is not known *a priori*. Thus, there is an urgent need for alternative MRI approaches that are safer and more efficient.

An attractive alternative approach is ^{19}F NMR.[12] The only natural isotope of fluorine, ^{19}F, possesses favorable physicochemical properties (spin = 1/2, 100% abundance, relatively large magnetogyric ratio), which make ^{19}F NMR almost (*ca.* 83%) as sensitive as ^{1}H NMR. Moreover, ^{19}F is essentially absent from any biological tissue, so any exogenous fluorine-containing compound would be detected as a "hot spot on a cold background". These favorable properties open the way to using fluorinated molecules as reporter agents. The combination of ^{1}H- and ^{19}F-images in MRI analysis would generate a full picture of the sample.[13−15] On one hand, due to the abundance of protons in the body, ^{1}H NMR is suitable for collecting information about the body and is, therefore, a valuable tool for disease diagnostics. ^{19}F MRI, on the other hand, is a tracer-type technology and is suitable for collecting information about an administered drug, i.e., where and in what form and amount the drug is present in the body. Therefore, it has the potential to become a valuable tool for image-guided drug therapy.

Although ^{19}F MRI is only four years younger than ^{1}H MRI, it is still not in clinical use.[16,17] The progress of ^{19}F MRI has been delayed by the lack of suitable imaging agents.[14] For more than three decades, the only agents used for ^{19}F-based imaging have been perfluorocarbon (PFC) emulsions.[17−21] However, PFC emulsions suffer from severe drawbacks as imaging agents, including heterogeneity, instability, split ^{19}F NMR signals, complex formulation procedure, and, most importantly, the prolonged retention of the agents within organs for months or longer.[22,23]

All the aforementioned shortcomings of PFC-based imaging agents can be avoided if a stable, hydrophilic molecule with a single ^{19}F signal from multiple fluorine atoms can be developed. As part of the program on the development of cancer-oriented theranostic agents, we have synthesized a construct containing a chemotherapeutic agent fluoropyrimidine attached to a targeting macromolecule (polyethyleneimine, PEI) and carrying polyunsaturated fatty acid (linoleic acid, LA) as a homing device and urocanic acid as a drug releasing agent (Figure 1).

Several fluoropyrimidine derivatives are currently being developed or are already used as anticancer drugs in standard chemotherapeutic regimens.[24−35] Gemcitabine (2,2′-difluorodeoxyribofuranosylcytosine, dFdC) is an analog of deoxycytidine with two fluorine atoms inserted into the deoxyribofuranosyl ring instead of hydrogens.[24] Clinically, dFdC has been

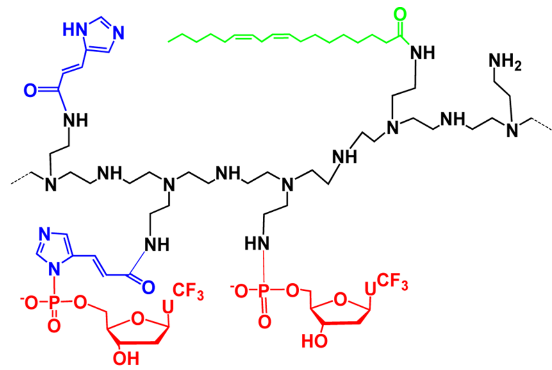

Figure 1. Schematic presentation of the multifunctional theranostic construct. Carrier (black) − PEI: charge-mediated cellular uptake. Effector (red) − pTFT: chemotherapeutic agent; ^{19}F-based magnetic resonance molecular imaging probe. Homing device (green) − linoleic acid: high affinity binding to alpha-fetoprotein receptor expressing cells. Releasing agent (blue) − urocanic acid: pH-responsive drug release. In the structure, the positions of linoleic acid, pTFT, and urocanic acid attachment are tentative. Note that pTFT can conjugate with both primary amino groups of PEI and nitrogens of imidazolyl group of urocanic acid attached to PEI.

used as a first-line chemotherapeutic agent for a wide variety of cancers including nonsmall cell lung cancer and pancreatic cancers.[25−27] Despite the clinical success of dFdC, the chemotherapeutic efficacy of the drug is greatly limited by its short plasma half-life (9−13 min in humans) and adverse toxicity (myelosuppression).[27,28]

5-Fluorouracil (5-FU) has been in clinical use for cancer treatment for over 45 years.[29,30] For example, 5-FU-based therapy is a part of the standard treatment regimen for colorectal and breast cancer.[31] The combination of 5-FU with leucovorin was reported to increase survival of cancer patients, but the examples of resistance to the drug are plenty.[32]

Another type of oral formulation, TAS-102, is currently in a phase II clinical trial for colorectal cancer.[33,34] The formulation contains 5-trifluoromethyl-2′-deoxyuridine (TFT, trifluorothymidine)[35] in combination with a specific inhibitor of thymidine phosphorylase. TFT is a more potent antitumor agent than 5-FU because it induces higher levels of cell death and does not cause an autophagic survival response in the cancer cell lines.[36] This provides a strong molecular basis for further application of TFT in cancer therapy.

Along with its beneficial properties as a chemotherapeutic agent, TFT is a promising imaging agent. It contains a trifluoromethyl group, which provides a number of advantageous properties for MRI. First, the free rotation of the trifluoromethyl group assures that the NMR line remains narrow, even if the agent is a part of high molecular weight complexes. Isolation of the α-fluorines from hydrogens and other nuclei with a nonzero spin assures that fluorine signals are not split into multiplets by couplings to ^{1}H nuclei. Such splittings would either lead to a loss in sensitivity or require the use of ^{1}H decoupling in the ^{19}F-detected spectrum, which is associated with heating in biological samples. In a trifluorothymidine molecule, three fluorine nuclei of the trifluoromethyl group are magnetically equivalent. The same chemical shifts of the three fluorines at the methyl position allows avoiding image artifacts. In comparison with 5-FU, for example, TFT offers the advantage of higher sensitivity. By substituting three hydrogens of the thymidine methyl group with fluorines, a 3-fold increase in concentration of the detected nucleus

relative to the amount of the administered pyrimidine analog is achieved. Thus, for the same number of TFT and 5-FU molecules present at a tumor site in the tissues, an NMR signal from the trifluoromethyl group of TFT is expected to be three times stronger. Higher sensitivity allows the detection of lower concentrations of the anticancer agent, reducing the required concentrations and thus alleviating toxicity issues.

In this work, we suggest to use TFT as a part of anticancer theranostic vector−drug construct. The construct contains branched polyethyleneimine modified with linoleic acid and conjugated with trifluorothymidine via an acid-sensitive phosphamide bond. If administered as a single agent, TFT is known to be rapidly degraded in the human body (its plasma half-life is less than 20 min).[37] By conjugating TFT with PEI, the therapeutic index of the drug can be greatly improved, since the polymer protects TFT from renal clearance and, therefore, prolongs its circulation half-life. In addition, the enhanced permeation and retention effect of the macromolecular drug will allow preferential accumulation of the drug in tumor tissues. It will contribute to the local drug uptake and ensure the release of the drug in the acidic environment of the tumor.

Commercially available PEI has been used as a polymeric carrier for macromolecular drug preparations by a number of research groups.[38] Due to the negatively charged cell surface, polycationic polyethyleneimine and its derivatives generally display sufficient association and internalization rates. As a DNA carrier, PEI has already demonstrated significant potential in gene therapy showing high transfection efficiency both *in vitro* and *in vivo*. However, acute toxicity caused by PEIs slowed clinical applications of the polymer. *N*-Acylation of the polymer helps to reduce toxicity and enhance the transfection efficiency of PEI.[39] A series of PEI-based nanoparticles with a varying degree of imidazolyl substitution were synthesized.[40] The cytotoxicity of nanoparticles was shown to decrease with increasing imidazolyl content. The transfection efficiency of PEI (25 kDa), which is a gold standard for cationic polymer-based DNA delivery systems, was also improved by 3- to 4-fold upon substitution with imidazole and lauric acid.[40] Since the pK_a of imidazolyl group is within the acidic range of endosome lumen (pH 5.5−6.5), the group acts as a proton sponge inside the endosome compartment. Following endocytosis, the DNA−polymer complexes were shown to be released into cytoplasm by means of the proton sponge property of imidazole groups, which were incorporated into the polymeric vector in the form of histidine residues.[40−42]

In the present work, we used branched PEI modified with linoleic acid (PEI-LA) as a carrier. To enhance the release of the drug from the conjugate in the targeted cells, we coupled PEI-LA polymer with urocanic acid, which bears an imidazole ring and thus can form an acid-labile P−N bond with pTFT. In this case, the drug can be released from the PEI-LA-urocanic acid carrier in the endosomes due to the endosomal rupture through proton sponge mechanism.

The drugs could be selectively transported into the cancerous cells using vectors in order to avoid dangerous side effects. The working principle of a vector consists of using the affinity of certain substrates for metabolite receptors. Indeed, cancer cells are subjected to higher metabolic rates compared to normal cells. Faster metabolism results in hypoxic environment inducing anaerobic metabolism that lowers the pH of cancer cells. Therefore, cancer cells overexpress receptors that attract primary metabolites (peptides, polysaccharides, fatty acids, etc.). Incorporation of linoleic acid residues into polyethyleneimine−nucleic acid conjugates provides their interaction with blood plasma proteins,[43] which can cause the delivery of such conjugates in a cancer tissue because of overexpression of special receptors in the tumor cell membrane.[44] The results obtained[45,46] showed that the coupling of drugs with polyunsaturated fatty acids improves their *in vitro* toxicity as well as selectivity against malignant lymphocytes as compared with quiescent nonproliferating cells. Therefore, previous works have provided evidence that (a) the entry of fatty acids into cells is regulated and facilitated by α-fetoprotein (AFP) through its interaction with specific receptors[46−49] and (b) an AFP/AFP-receptor pathway may be activated in neoplastic cells of various origin as well as in normal lymphocytes undergoing blastic transformation.[48,49] In this sense modified PEI (Figure 1) has a dual effect, as a vehicle of drug delivery and as a compound which enhances the bioavailability of TFT in cancer cells.

RESULTS

Synthesis and Characterization of Acylated Polymers.

Lipid-Substituted 25 kDa PEI. PEI is a cationic polymer with endosomolytic activity.[38] The polymer's ability to facilitate the endosome lysis is presumably a result of its high buffering capacity at the acidic endosomal pH. Branched PEI contains primary and secondary amino groups, which can be used for the attachment of a desired targeting ligand, either directly or via a spacer. These properties make branched PEI ideally suitable for the development of multifunctional drug−vector ensembles for anticancer agent delivery. In this study, PEI (25 kDa) was sequentially modified by linoleic acid and urocanic acid (to introduce imidazolyl groups into the polymer). The scheme for preparation of the modified polymer PEI-LA-UA is given in Figure 2.

The expected ratio of primary/secondary/tertiary amines in branched polyethylenimine was reported as 1:2:1.[50] At the same time, for commercially available compounds experimental measurements give values that are close to a 1:1:1 ratio, which

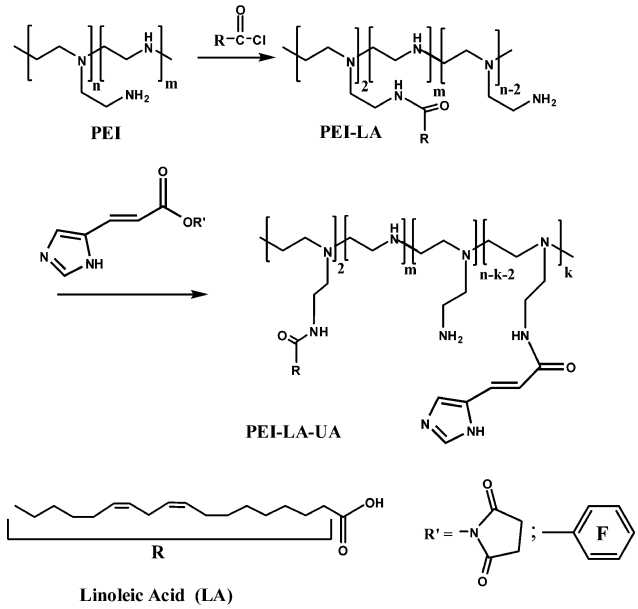

Figure 2. Synthesis of acylated polyethylenimine using linoleic acid chloroanhydride and active esters of urocanic acid (*N*-hydroxysuccinimide or pentafluorophenyl).

dx.doi.org/10.1021/bc3006072 | *Bioconjugate Chem.* 2013, 24, 780−795

indicates that the polymer has an even more branched structure.[51,52] To estimate the content of primary, secondary, and tertiary amino groups in the PEI preparation used in this work, we analyzed the sample using ^{13}C and ^{1}H NMR spectroscopy. The ^{1}H NMR signals for the protons of methylene groups attached to primary (-CH_2-NH_2, $\delta \sim 3.05$ ppm), secondary (-CH_2-NH-CH_2-, $\delta \sim 2.89$ ppm), and tertiary ($N(-CH_2-)_3$, $\delta \sim 2.71$ ppm) amino groups in PEI were observed (Figure S1 in Supporting Information). However, these ^{1}H NMR signals were not resolved well enough to allow a quantitative analysis. According to the ^{13}C NMR data, the content of primary, secondary, and tertiary amino groups in PEI were found to be ~26%, ~37%, ~37%, respectively. Correspondingly, ~366 amino groups per polymer molecule are available for acylation (63% of 581 amino groups per PEI molecule). This preparation of branched 25 kDa PEI was acylated using linoleic acid chloroanhydride (Figure 2, PEI−LA conjugate).

The synthetic procedure was adapted from Neamnark et al.[53] Detailed synthetic procedures are given in Supporting Information. The conjugation of the linoleic acid to PEI was confirmed by ^{1}H NMR spectroscopy (Figure S1 in Supporting Information). It was estimated that about 0.35% of amino groups of PEI were acylated with LA (2 LA residues per polymer molecule).

Interaction of Human α-Fetoprotein and Albumin with Polyunsaturated Acid and Its PEI−LA Conjugate. It is known that, in blood, fatty acids are mostly bound to serum albumin.[54] α-Fetoprotein (AFP) is considered to be the fetal form of albumin.[43] In addition, the level of AFP increases in cases of tumor development.[43,44] As compared with albumin, which binds mainly saturated and monoene fatty acids, AFP from different species is known to have affinity to polyene fatty acids.[55] To test the effect of PEI on binding of polyunsaturated LA by human serum albumin (HSA) and AFP, we calculated apparent association constants (K_a) for protein-LA or protein-PEI-LA complexes using the method of fluorescent titration. Unsurprisingly, the complex of the fatty acid conjugate with AFP was 2 orders of magnitude more stable than that with HSA (Table 1). In addition, it was observed that the covalent attachment of LA to PEI resulted in just a slight change in the stability of the protein−fatty acid complex for both HSA and AFP (Table 1).

Table 1. Apparent Association Constants between Serum Albumin (HSA) or α-Fetoprotein (AFP) and Linoleic Acid and Its PEI Conjugate[a]

sample code	$K_{a(AFP)} \times 10^{-5}$ M^{-1}	$K_{a(HSA)} \times 10^{-5}$ M^{-1}
LA	40 ± 2	5.4 ± 0.4
PEI-LA	13 ± 2	0.1 ± 0.01

[a]Each value represents the mean of three independent determinations. Standard deviations were always less than 15% of the mean.

Imidazolyl-PEI-LA Modified Conjugates. To introduce imidazolyl moieties into PEI-LA, primary and secondary amino groups of the fatty acid-modified polymer were acylated with urocanic acid (UA) residues. The PEI-LA-UA conjugate was synthesized using *N*-hydroxysuccinimide activated ester of UA, which was obtained by a classic peptide type coupling using dicyclohexylcarbodiimide (DCC) as an activating agent (Figure 2). Alternatively, the following two-step procedure for PEI-LA-UA preparation was employed: urocanic acid was converted into an activated pentafluorophenyl ester intermediate using $Ph_3P/(PyS)_2$ as an activating agent followed by the reaction of the activated ester with the amino groups of PEI-LA (Figure 2). The extent of imidazolyl groups' incorporation into the polymer was determined using ^{1}H NMR spectroscopy and is given in Table 2.

Table 2. Extent of Incorporation of Imidazolyl Groups into PEI-LA

	mol UA/mol PEI	
activated ester used	aimed extent[a]	achieved extent
N-Hydroxysuccinimide ester	40	30
	60	40
	100	80
Pentafluorophenyl ester	40	25
	60	30
	100	70

[a]The aimed extent of incorporation corresponds to the excess of UA activated ester with respect to the polymer.

The results demonstrated that the extent of the polymer modification increased with the increasing molar ratios of the acylating reagent to the polymer. All of the obtained preparations of PEI-LA-UA were found to be soluble in pure water. We intended to keep the extent of the polymer labeling with imidazolyl groups relatively low (~5.3 mol % of modified amino groups in PEI-LA) in order not to compromise the primary amino groups of PEI-LA-UA conjugate necessary for further pTFT incorporation.

The imidazolyl-modified PEI conjugate was isolated from the low-molecular reactants by centrifugal filtration. To ensure that this procedure allowed successful removal of free urocanic acid, control experiments were performed where urocanic acid alone and in the mixture with PEI was passed through the same purification steps as the PEI-LA-UA reaction mixture. Lyophilization of the retentate yielded no urocanic acid detectable by ^{1}H NMR spectroscopy and UV−vis spectroscopy (data not shown). Overall, the yield of PEI-LA-UA conjugate was 87%.

The ^{1}H NMR spectrum of the obtained PEI-LA-UA conjugate is given in Figures 3B and S2 (Supporting Information). For comparison, the spectrum of the mixture of PEI with UA is also included (Figure 3A). In the spectra of the conjugate, the signals corresponding to the protons of PEI methylene groups and the protons of UA were observed at 2.4−3.6 ppm and 6.48−7.87 ppm, respectively, thus indicating the successful conjugation of urocanic acid to PEI-LA (Figures 3B and S2 in Supporting Information). The chemical shifts of the protons of imidazolyl moiety in PEI-LA-UA accord well with those for UA (Figure 3A). At the same time, the presence of amido group in the conjugated UA caused the downfield shift of the signals for UA protons, as compared to those of the free acid. In addition, the line width for the PEI-LA-UA signals was significantly different from that for UA (*cf.* Figures 3A,B and S2 in Supporting Information). The ^{1}H NMR spectra were not resolved well enough for the calculation of the coupling constants of the spin system and the quantitative determination of the percentage of primary and secondary amides in the polymer samples to be performed. It is interesting to note that the spectra of the PEI-LA-UA conjugates obtained via activated *N*-hydroxysuccinimide or pentafluorophenyl esters of UA were

dx.doi.org/10.1021/bc3006072 | *Bioconjugate Chem.* 2013, 24, 780−795

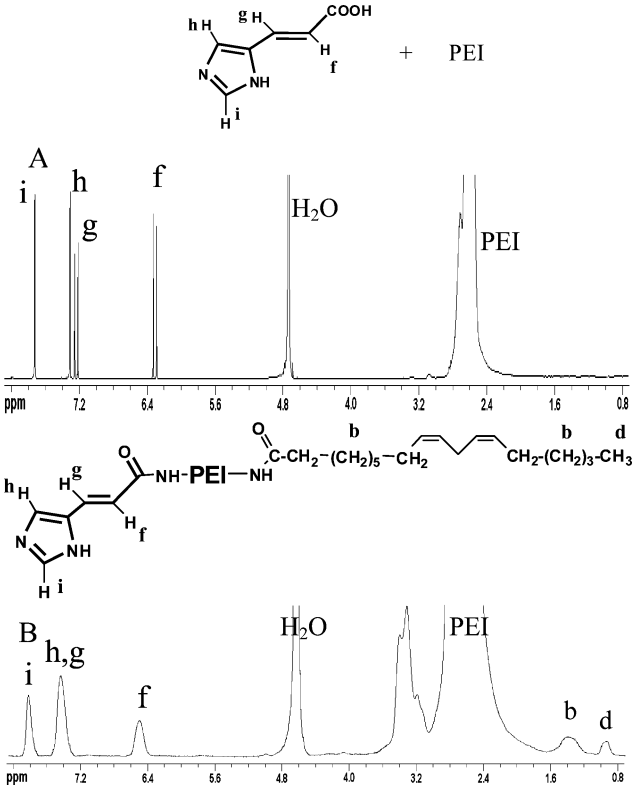

Figure 3. ^{1}H NMR spectra of PEI + UA (A) and PEI-LA-UA conjugate obtained via *N*-hydroxysuccinimide activated ester (B) in D_2O. Signals in the spectra A and B have been assigned to protons (b through i) of the structures shown above the spectra.

somewhat different (compare Figures 3B and S2 in Supporting Information). If urocanic acid was activated via a pentafluorophenyl active ester intermediate using $Ph_3P/(PyS)_2$, the ^{1}H NMR spectrum of the polymer conjugate contained a double set of signals for protons of −CH═CH− fragment (Figure S2 in Supporting Information). These signals can correspond to the *trans*-urocanic acid moiety (H-f, H-g) and *cis*-urocanic acid moiety (H-f′, H-g′). It is known that the ^{1}H resonances of *cis*-urocanic acid are significantly different from that for *trans*-urocanic acid.[56,57] In the spectrum of PEI-LA-UA obtained via *N*-hydroxysuccinimide ester of UA (Figure 3B), the signals for the protons of *cis*-urocanic acid moiety were not present.

Figure 4 illustrates the UV absorption spectra of PEI-LA-UA (spectrum A) and UA (spectrum D) recorded at pH 6.4.

It can be seen that the polymer conjugate absorbs in the higher wavelength region than free UA and with a larger molar absorptivity ε (for the *trans*-form of urocanic acid $\varepsilon = 1.88 \times 10^4$ M^{-1} cm^{-1} at 278 nm, and for the PEI-LA-UA conjugate, $\varepsilon = 5.76 \times 10^5$ M^{-1} cm^{-1} at 285 nm; $\lambda_{min} = 245$ nm, $\varepsilon = 1.65 \times 10^5$ M ^{1} cm ^{1}). The variation of the UV spectrum for *trans*-UA with pH has been well documented.[58] The UV absorption characteristics of PEI-LA-UA conjugate showed a virtually identical variation with pH to that of UA except for the higher value for the molar absorptivity across the spectrum (data not shown).

Synthesis and Characterization of Phosphorylated PEI Conjugates (PEI-LA-pTFT and PEI-LA-UA-pTFT). To introduce an anticancer nucleotide antimetabolite pTFT into PEI-LA (Figures S3 and S4 in Supporting Information) and PEI-LA-UA (Figure 5) polymers, we used 4-(*N*,*N*-dimethylamino)-pyridine derivative of pTFT (DMAP-pTFT). Detailed

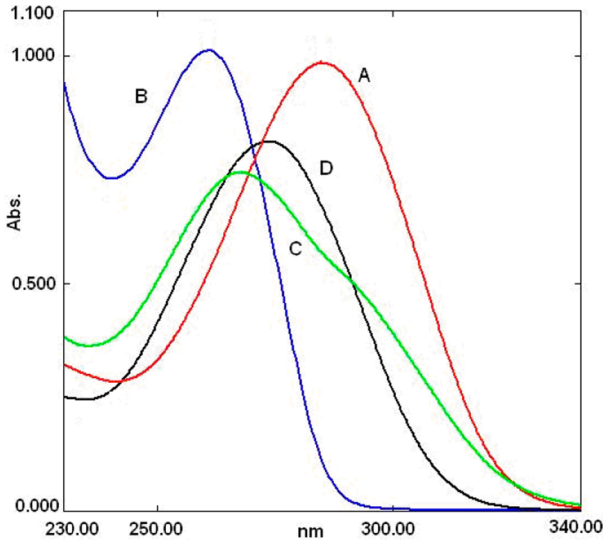

Figure 4. Electronic absorption spectra of the PEI-LA-UA conjugate (spectrum A), PEI-LA-pTFT conjugate (spectrum B), PEI-LA-UA-pTFT conjugate (spectrum C), and UA (spectrum D) in an aqueous solution, pH 6.4.

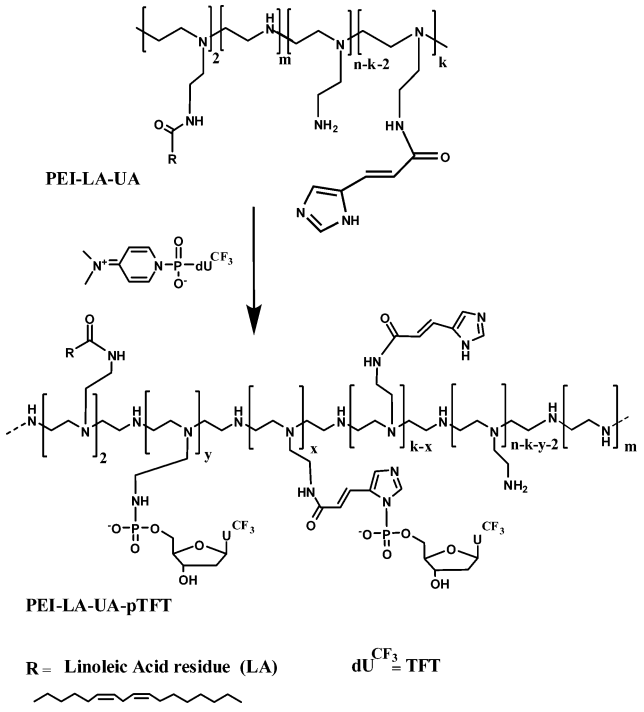

Figure 5. Scheme for the synthesis of the PEI-LA-UA-pTFT conjugate.

synthetic procedures are given in Supporting Information. The procedure for the synthesis of a phosphorylating derivative of pTFT (DMAP-pTFT) was adapted from Godovikova et al.[59]

To obtain polymers with different degrees of substitution with the anticancer agent pTFT, we varied the pTFT:polymer ratio in the reaction mixtures. The aimed and achieved substitution degrees are given in Table 3. The results showed that the extent of the polymers modification increased with the increasing molar ratios of the phosphorylating reagent to the polymer. All of the obtained conjugates were found to be soluble in pure water. However, aggregation was detected for PEI-LA-UA-pTFT-70. We intended to keep the extent of

dx.doi.org/10.1021/bc3006072 | *Bioconjugate Chem.* 2013, 24, 780−795

Table 3. Extent of Modification of PEI-LA and PEI-LA-UA Conjugates with pTFT

samples	mol pTFT/mol PEI	
	aimed extent[a]	achieved extent
PEI-LA-pTFT-20	30	20
PEI-LA-pTFT-40	50	40
PEI-LA-pTFT-70	90	70
PEI-LA-UA-pTFT-40	50	40
PEI-LA-UA-pTFT-70	100	70

[a]The aimed extent of incorporation corresponds to the excess of DMAP-pTFT with respect to the polymer.

modification relatively low (~7 mol % of amino groups in PEI-LA-UA-pTFT), in order to avoid formation of micelles.

The PEI-LA-pTFT and PEI-LA-UA-pTFT conjugates were isolated by centrifugal filtration with a ~75% yield. The chosen purification method was shown to successfully separate the excess of low molecular weight reactant from the polymer. Indeed, the retentate after centrifugal filtration of free pTFT solution and its mixture with PEI did not contain pTFT, according to ^{31}P, ^{1}H, and ^{19}F NMR spectroscopy (data not shown).

The TFT-containing PEI conjugates were further characterized by ^{31}P, ^{1}H, and ^{19}F NMR. It is known that in nucleotide derivatives the chemical shift of the 5′-phosphate group depends on the medium effects.[60] The chemical shifts for the ^{31}P NMR signal of the phosphate monoester group in aqueous solutions depend on pH in the ionization region of this group and can vary within a ~4 ppm interval. Therefore, we detected the ^{31}P NMR spectrum of the nonactivated pTFT mixed with PEI-LA as a control. In the control spectrum, only the signal at ~4 ppm corresponding to the phosphate monoester was observed (Figure 6A). At the same time, this signal was absent in the ^{31}P NMR spectra of PEI-LA-pTFT (Figure 6B) and PEI-LA-UA-pTFT (Figure 6C). Instead, the signal with a chemical shift at ~9 ppm appeared in both spectra. It is known that the

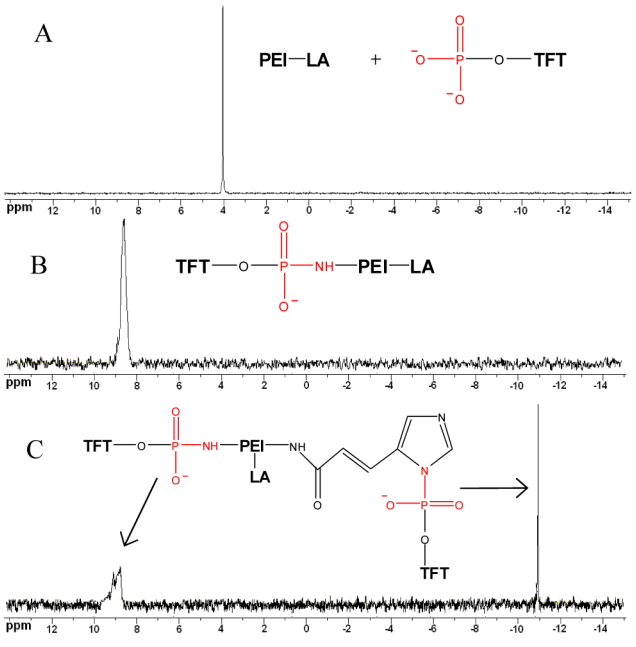

Figure 6. ^{31}P NMR spectra of pTFT (A), PEI-LA-pTFT (B), and PEI-LA-UA-pTFT (C) conjugates in D_2O.

signals for phosphorus atom in monoamides of phosphate monoesters obtained with primary (secondary) amines are shifted downfield in comparison with mononucleotides.[60] Therefore, the signals at ~9 ppm can be attributed to the phosphorus in an aliphatic amidophosphate group, which indicates the successful conversion of pTFT into the corresponding polymer conjugates.

In addition, in the ^{31}P NMR spectrum of PEI-LA-UA-pTFT the peak with $\delta \sim -11$ ppm was detected (Figure 6C). Signals in this region are characteristic of the phosphamide bonds formed with a nitrogen atom included in the aromatic π-system (*e.g.*, the signals for imidazolides of mononucleotides in D_2O have chemical shifts in the range between −10 and −11 ppm).[60] Therefore, the ^{31}P NMR data speaks in favor of the attachment of some pTFT residues to the imidazolyl moieties of UA introduced into PEI. This fact was also confirmed by the kinetic experiments for acid-sensitive release of pTFT from PEI-LA-UA-pTFT conjugate at different pH (discussed below).

The synthesis of PEI-LA-pTFT and PEI-LA-UA-pTFT conjugates was further confirmed by ^{1}H NMR (Figure 7) and ^{19}F NMR spectroscopy. The ^{1}H NMR spectra of the conjugates contained signals for PEI protons at $\delta \sim 2.2-3.6$ ppm (Figure 7B,C). In addition, the singlet peak for the aromatic proton of the nucleotide residue (H-6, H-o) was observed at $\delta \sim 8.2$ ppm; a proton H-1′ (H-n) of deoxyribose moiety produced a signal at $\delta \sim 6.3$ ppm; and the signals for H-4′ (H-k), the signals for H-3′ (H-l), and the signals for H-5′(H-j) appeared markedly at $\delta \sim 4.5$ ppm, $\delta \sim 4.2$ ppm, and $\delta \sim 4.0$ ppm, respectively. The signals corresponding to the protons of UA were observed in the range of 6.38−7.70 ppm in the ^{1}H NMR spectrum of PEI-LA-UA-pTFT as well (Figure 7C).

In the ^{19}F-NMR spectra of PEI-LA-pTFT and PEI-LA-UA-pTFT conjugates, several overlapping signals appeared at *ca.* 101.5 ppm (D_2O). The chemical shifts of conjugates were essentially coincident with that of pTFT. The signals were shifted downfield by ~58 ppm from the ^{19}F NMR signal of NaF. The line width in the spectra of the polymer conjugates was significantly larger than that for small molecular weight fluorinated compounds (*e.g.*, for pTFT, the line width was ~20 Hz; for PEI-LA-UA-pTFT it was ~140 Hz).

The UV absorption spectra of the PEI-LA-pTFT and PEI-LA-UA-pTFT conjugates recorded at pH 6.4 are demonstrated in Figure 4 (spectra B and C, respectively). It can be seen that the conjugates absorb in the same wavelength region as TFT (for PEI-LA-pTFT-40, $\varepsilon = 3.3 \times 10^5$ M^{-1} cm^{-1} at 262 nm; for PEI-LA-UA-pTFT-40, $\varepsilon = 8.82 \times 10^5$ M^{-1} cm^{-1} at 267 nm; $\lambda_{min} = 235$ nm, $\varepsilon = 4.4 \times 10^5$ M^{-1} cm^{-1}). The presence of UA residue in the PEI-LA-UA-pTFT conjugate was also proved by the appearance of the characteristic inflection at 291 nm along with the single maximum at 267 nm (Figure 4C). The absorption maximum for the TFT-containing polymer conjugates was blue-shifted in comparison with the initial modified polymers due to the presence of the pTFT moiety (Figure 4, compare spectra A and C).

Release of pTFT from PEI-LA-pTFT and PEI-LA-UA-pTFT Conjugates. It is known that phosphorylated imidazole is unstable at pH < 5.[61] Mono- and oligonucleotide derivatives containing the P−N bond with aliphatic amino group are much more stable under the same reaction conditions. To additionally confirm that at least some pTFT moieties were attached to the polymer via imidazolyl residues of the introduced urocanic acid, we studied the acid sensitivity of phosphamide bonds in the TFT-containing polymer conjugates by UV−vis spectros-

dx.doi.org/10.1021/bc3006072 | *Bioconjugate Chem.* 2013, 24, 780−795

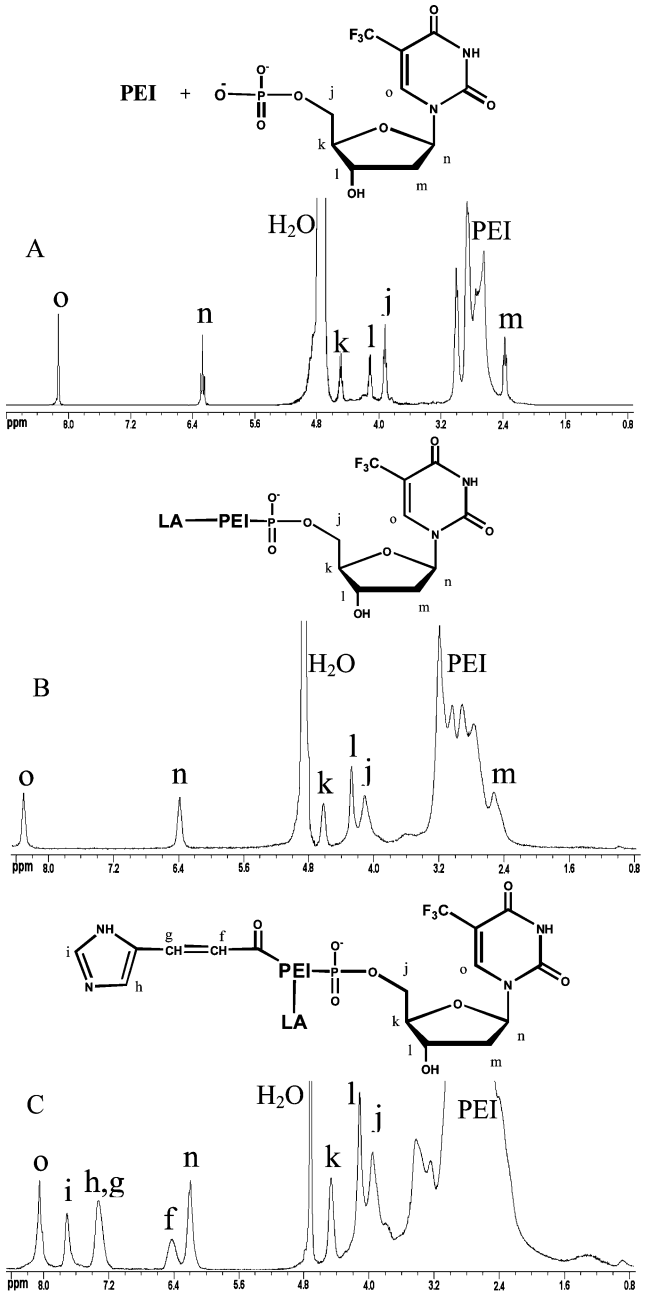

Figure 7. ^{1}H NMR spectra of PEI mixed with pTFT (A), PEI-LA-pTFT conjugate (B), and PEI-LA-UA-pTFT conjugate (C) in D_2O. Signals in the spectra correspond to protons labeled (f through o) in the structures shown above the spectra.

copy (Figure S5 in Supporting Information) and high-resolution ^{31}P NMR spectroscopy (Figure 8). It was expected that hydrolysis of the polymer conjugates would produce a small molecular weight fluorinated compound (i.e., pTFT) and a demodified polymer, which could be separated using centrifugal filtration. As a result of pTFT release, the absorbance at 267 nm (A_{267}) of the polymeric fraction upon filtration would decrease, providing a means to evaluate the degradation of the conjugates. Indeed, when PEI-LA-UA-pTFT was incubated at pH 5.0 or 7.0, the value of A_{267} decreased over time. However, the change in absorbance was slower at pH 7.0 than at pH 5.0, indicating that the hydrolysis of the conjugate was pH-dependent, faster at lower pH. In contrast, the

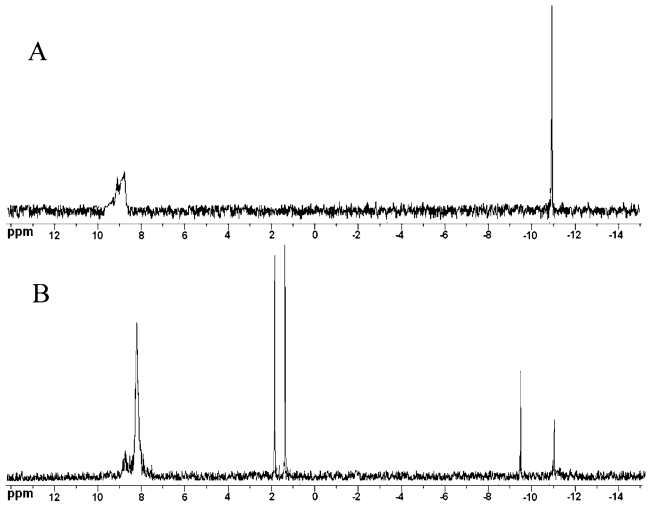

Figure 8. ^{31}P NMR spectra of PEI-LA-UA-pTFT conjugate before (A) and after its incubation at pH 5.0, 37 °C for 24 h (B).

absorbance of the polymeric fraction upon the hydrolysis of PEI-LA-pTFT did not change, whether the polymer conjugate was incubated at pH 5.0 or at pH 7.0. Thus, the PEI-LA-pTFT was stable at the pH tested. The percentage of hydrolysis for the conjugates as a function of time is shown in Figure S5 (Supporting Information). At pH 5.0, ∼13% of PEI-LA-UA-pTFT conjugate was hydrolyzed within 11 h of incubation, and after 72 h, the percentage of hydrolysis increased to 70%. In contrast, at pH 7.0, only ∼8% of the conjugate degraded within 11 h of incubation. The hydrolysis percentage for PEI-LA-pTFT at pH 5.0 within 72 h was negligible (only ∼0.1% of PEI-LA-pTFT was hydrolyzed).

As it was mentioned above, the difference in the chemical shifts for the phosphorus in phosphate and in phosphamide groups allowed us to distinguish between pTFT-free and TFT-containing polymers. Therefore, high-resolution ^{31}P NMR spectroscopy was used to further study the pH-dependent degradation of PEI-LA-UA-pTFT conjugate. Indeed, the integrals of the signals for aliphatic phosphamides and phosphamides formed with imidazolyl groups in the polymer molecule (chemical shifts of ∼9 ppm and −11 ppm, respectively) decreased upon incubation of PEI-LA-UA-pTFT at pH 5.0 (Figure 8). At the same time, the integral of the signal for phosphate monoesters (δ ∼ 2 ppm) gradually increased, indicating the disappearance of the PEI-LA-UA-pTFT conjugate and the appearance of pTFT.

The appearance of the peak at δ −9.5 ppm in the ^{31}P NMR spectrum of the PEI-LA-UA-pTFT hydrolysis mixture indicated the conversion of pTFT into symmetrically disubstituted pyrophosphates (Figure 8B). It is known that symmetrically disubstituted pyrophosphates produce singlet peaks in ^{31}P NMR spectra, which are shifted in respect to phosphomonoester signal upfield and appear at approximately −10 ppm.[60] It seems reasonable to suggest that pyrophosphates may be formed by interaction of mononucleotide imidazolides with the mononucleotides released from the PEI-LA-UA-pTFT conjugate.

***In Vivo* Spectroscopy.** One of the powerful noninvasive analytical techniques is *in vivo* MR spectroscopy.[62] To evaluate the potential of ^{31}P MRS *in vivo*, we visualized PEI-LA-pTFT conjugate administered to mice by intramuscular injection of

dx.doi.org/10.1021/bc3006072 | *Bioconjugate Chem.* 2013, 24, 780−795

PEI-LA-pTFT solution (13 mM, calculated as the concentration of phosphate groups; 0.3 mL) (Figure 9).

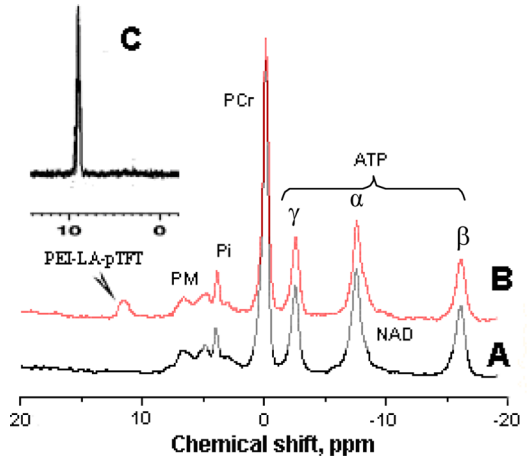

Figure 9. *In vivo* ^{31}P MRS spectra of mouse muscle tissue before (A) and after (B) the intramuscular injection of PEI-LA-pTFT. The spectra were recorded using a surface coil. A NaCl/H_2O solution of the conjugate (13 mM, calculated as the concentration of phosphate groups; 0.3 mL) was used for injection. The number of signal accumulations NS = 10 000. PM – phosphomonoester; P_i – inorganic phosphate; PCr – phosphocreatine; ATP – adenosine 5′-triphosphate; NAD – nicotinamide adenosine dinucleotide. (C) ^{31}P NMR spectrum of PEI-LA-pTFT.

After injection of PEI-LA-pTFT, a new resonance at *ca.* 12 ppm arose in the ^{31}P NMR spectrum of the mouse muscle tissue (Figure 9, compare spectra A and B). The chemical shift of this signal was coincident with that of PEI-LA-pTFT (Figure 9C) and is shifted by ~6 ppm downfield from the signal of inorganic phosphate. After injection of PEI-LA-pTFT into mice muscle tissue, the concentration of the conjugate remained constant within the first 5 min and then slightly decreased within 1–2 h after administration, as demonstrated by the changes in the intensity of the amidophosphate signal (Figure 10).

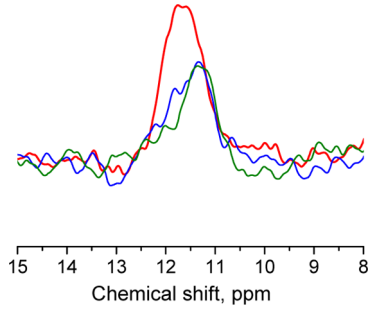

Figure 10. ^{31}P MRS spectra (the region around $\delta \sim 11.5$ ppm) of a mouse muscle tissue obtained using a surface coil upon administration of one dose of 0.1 μmol of the PEI-LA-pTFT conjugate 5 min (red), 50 min (blue), and 75 min (green) after injection.

The ability of *in vivo* ^{31}P MRS to distinguish the signal for amidophosphate from the signals for endogenous phosphorus-containing compounds makes this technique suitable for the analysis of amidophosphate-containing polymers *in vivo*. Thus, such conjugates may serve as useful molecular probes for evaluation of tissue perfusion and for the future investigation of the pharmacodynamic and pharmacokinetic properties of the amidophosphate-containing anticancer conjugates.

***In Vitro* Studies.** The binding and uptake of PEI-LA-pTFT and PEI-LA-UA-pTFT conjugates labeled with fluorescein isothiocyanate (FITC) were studied in MCF-7 human breast adenocarcinoma cells, which are characterized by a high level of AFP receptor expression (300 000 receptors per cell).[63] The fluorescent microscopy was utilized to investigate intracellular localization of the conjugates. Both types of FITC-labeled conjugates are characterized by a high level of accumulation in the cells (Figure S7 in Supporting Information).

The cytotoxicity of PEI and the obtained polymer conjugates was investigated using the MTT assay.[64] The polymer solutions were incubated with MCF-7 human breast adenocarcinoma cells for 72 h. It is known that cationic polymers such as PEI are toxic due to their strong interactions with plasma membrane or interactions with negatively charged cell components.[38,65−67] Indeed, PEI showed the highest toxicity among a series of polycations tested in L929 mouse fibroblasts, and the effect depended upon exposure time and concentration of the polycation.[67] In addition, studies on poly(L-lysine) and PEI showed that primary and secondary amines increased toxicity, while tertiary amines reduced toxicity.[68] In the current study, PEI showed IC_{50} value of 0.49 μM after 72 h incubation with MCF-7 cells. Substitution of PEI with LA reduced cytotoxicity of the polymer, which had an IC_{50} of 0.67 μM after 72 h incubation (Table 4).

Table 4. IC_{50} Values for PEI and Its Derivatives after 72 h Incubation with MCF-7 Cells

sample	IC_{50} (72 h)[a] (μM)
PEI	0.49 ± 0.02
PEI-LA	0.67 ± 0.03
PEI-LA-pTFT-20	0.32 ± 0.015
PEI-LA-pTFT-40	20% inh[b]
PEI-LA-pTFT-70	10% inh[b]
PEI-LA-UA-pTFT-40	0.43 ± 0.01

[a]The values mean ± SD were calculated from cell viability percentages obtained from MMT assay done in triplicate and repeated three times. Statistical significance of modified polymer compared to unmodified polymer using two-sample *t*-test is given. [b]When the cytotoxicity was low, the percent of inhibition of cell growth at the highest used concentration (0.8 μM) of the compound was determined.

In the present study, a series of PEI-based conjugates were synthesized with different degrees of TFT substitution. The cytotoxicity of the obtained polymer conjugates varied depending on the number of pTFT residues per polymer molecule (Table 4).

The conjugates with a pTFT substitution of 40 and 70 pTFT molecules per polymer molecule (conjugates PEI-LA-pTFT-40 and PEI-LA-pTFT-70, respectively) demonstrated reduced cytotoxicity, which can be explained by their reduced surface charge in comparison with the parent polymer. The trend is clearly reflected in the IC_{50} values, which demonstrate that the cells can tolerate greater amounts of substituted PEIs as the degree of pTFT substitution increases (Tables 3 and 4). The cell survival following the 72 h treatment with 0.8 μM solution of PEI-LA-pTFT with a pTFT/PEI molar ratio of 70 was higher than 90%.

As can be seen in Table 4, reducing the primary amine content of the PEI-LA conjugates lowered their toxicity, as

dx.doi.org/10.1021/bc3006072 | *Bioconjugate Chem.* 2013, 24, 780−795

compared to PEI. Cytotoxicity of the conjugates diminishes with the increase of phosphorylation degree due to the decrease in the amount of primary amino groups per polymer molecule. The PEI-LA-UA-pTFT-40 conjugate obtained in the present work is a prodrug, which needs to be hydrolyzed to produce active pTFT. Acid-sensitive hydrolysis, either extracellular or intracellular, of the imidazolyl phosphamide bond in the conjugate followed by the quick release of the cytotoxic antimetabolite should contribute to the increased cytotoxicity of the PEI-LA-UA-pTFT-40 conjugate. TFT induces higher levels of cell death and does not elicit an autophagic survival response in the cancer cell lines.[36] In contrast to imidazolyl amidophosphates, the aliphatic amidophosphates are relatively stable under physiological and slightly acidic conditions. Therefore, the antimetabolite cannot be easily released from the carrier in the case of PEI-LA-pTFT conjugates, which may limit the cytotoxic properties of the conjugates.

***In Vivo* Antitumor Activity.** To evaluate the *in vivo* antitumor activity of the PEI-LA-UA-pTFT conjugate, C57BL/6-tumor-bearing mice were treated with normal saline or PEI-LA-UA-pTFT solution. The body weights of mice that received various treatments were recorded. The drug was administered by i.p. injections three times at a single dose of 24 mg/kg on days 2, 4, and 6 after tumor transplantation (on day 1). Control animals received three corresponding injections of saline. The mice were weighed daily, and on day 8 they were decapitated, ascites was removed, weighed, the ascitic cells were counted, and the tumor-inhibitory activity of the polymer conjugate was assessed (Table 5).

Table 5. Effect of Normal Saline or PEI-LA-UA-pTFT-40 Conjugate on the Growth of Murine Krebs-2 Ascitic Carcinoma in C57BL/6 mice (n = 4)

	normal saline	PEI-LA-UA-pTFT conjugate
Initial body weight (average, g)	23.5	22.9
Final body weight with ascites, g	28.3 ± 1.1	21.9 ± 0.7
Final body weight without ascites, g	22.2 (94.5%)	20.8 (90.8%)
Mean weight of ascites, g	6.2 ± 1.1	1.1 ± 0.2
Tumor cell concentration (mln/mL of ascites)	47.5	3.3
Mean number of tumor cells per mouse (mln)	294.5	3.63
Tumor growth inhibition: by weight of ascites	-	~82.3%
Tumor growth inhibition: by tumor cell number	-	~98.8%

As seen in Table 5, tumors in mice treated with normal saline grew aggressively and uncontrollably, and the tumor weight reached 6.2 ± 1.1 g on day 8, *i.e.*, seven days after the first injection. In contrast, PEI-LA-UA-pTFT significantly inhibited the tumor growth compared with normal saline treatment. The mean size of tumors in mice that have been treated with the conjugate on day 8 was found to be significantly smaller (1.1 ± 0.2 g) than that in mice treated with normal saline. The ratio of the volumes of ascites from the drug-treated animals to that of control mice was 0.177, and the corresponding ratio for the number of tumor cells was 0.012, which allowed calculation of the tumor growth inhibition to be 98.9%.

The second experiment was performed to evaluate the effect of PEI-LA-UA-pTFT on the life span of the tumor-bearing mice. The animals were treated as in the previous experiment, but then were allowed to naturally die from tumors. Whereas mice of the control group lived for 8.9 ± 0.11 days after tumor transplantation, the conjugate-treated animals lived for 30.3 ± 3.12 days ($p < 0.001$), which is more than 3 times longer as compared to the control.

DISCUSSION

Nowadays, cancer chemotherapy depends heavily on cytotoxic antimetabolites, such as nucleoside analogs.[36,69−71] The initial studies evaluating the anticancer activity of a nucleoside analog TFT were conducted in the 1960s,[35] but further development of this agent was not undertaken because of its short half-life (12−18 min) in plasma and pronounced hematologic toxicity.[37,70] The metabolism of TFT in the body includes two stages: the cleavage of the nucleoside to the free base; and the conversion of the base into 5-carboxyuracil with the concomitant release of inorganic fluoride. Thymidine phosphorylase (TP) is the enzyme responsible for the degradation of TFT into its inactive form, 5-trifluoromethyluracil. In order to prolong the half-life of the drug in the body, a fluoropyrimidine formulation should be made resistant to the enzyme.

A type of TP-resistant fluoropyrimidine formulation, TAS-102, has recently been introduced and is now in phase II of clinical trials.[33] The formulation consists of TFT in combination with a specific inhibitor of TP (5-chloro-6-(2-iminopyrrolidin-1-yl)-methyl-2,4(1*H*,3*H*)-pyrimidine dionehydrochloride). The presence of the TP inhibitor results in a 3-fold increase in TFT serum concentrations. However, increased TFT concentration due to inhibition of TP does not necessarily lead to the increased delivery of the chemotherapeutic drug to the tumor cells. Thus, a more suitable and effective administration of nucleoside analogues is required for the successful treatment of cancer patients. Thereto, the therapeutic efficiency of anticancer nucleoside analogues strongly depends on their intracellular accumulation and conversion into 5′-mono- and triphosphates. If only a small portion of a nucleoside analog is converted into the corresponding nucleotide, the analog can cause high toxicity, and drug resistance can be developed, which eventually compromises the effectiveness of this therapy.[36] This problem could be solved by using phosphorylated forms of nucleoside analogues: mono- or triphosphates. Unfortunately, phosphorylated nucleosides applied alone are known to be hardly internalized by cells. To increase the internalization of this promising type of antimetabolites, efficient drug delivery vehicles are required. In the present study, a conjugate between a polymer carrier (PEI) and the active monophosphate form of TFT (pTFT) is reported for the first time.

Active targeting of tumor cells via receptor-mediated endocytosis is a promising approach to increase internalization of drugs by target cells and simultaneously to minimize the drug's action on healthy tissues.[72] In the current study, linoleic fatty acid (LA) was incorporated into PEI to provide the polymer-based drug ensemble with ligand competence. It has been proven that penetration of polyunsaturated fatty acids into cells is regulated and facilitated by interaction of AFP with specific receptors.[44] There exist as least two types of receptors for AFP. AFP uptake was demonstrated in neoplastic cells, such as breast/mammary carcinomas, hepatomas, neuroblastomas, lymphomas, and T and B cell malignancies.[44] Our results show that PEI acylated with linoleic acid chloroanhydride is bound to

dx.doi.org/10.1021/bc3006072 | *Bioconjugate Chem.* 2013, 24, 780−795

AFP about a hundred times more efficiently than to serum albumin (K_a = (13 ± 2) × 10^{-5} M and K_a = (0.1 ± 0.01) × 10^{-5} M, respectively). In addition, the results show that our modified polymer has lower toxicities in MCF-7 human breast adenocarcinoma cells compared to PEI (Table 4). Taken together, PEI-LA polymer demonstrated its promising potential as a drug carrier with low cytotoxicity and facilitated cellular uptake.

To use PEI-LA polymer as a platform for the delivery of anticancer drug pTFT into cells, we suggested a simple method to incorporate the drug into polymer. The amino groups of PEI were phosphorylated with DMAP-pTFT (Figure 5 and Supporting Information, Figure S2). Activation of the 5′-phosphate group was achieved as described in Godovikova et al.[59] using oxidative−reductive condensation with the pair $Ph_3P/(PyS)_2$ in the presence of 4-(*N*,*N*-dimethylamino)-pyridine. Interestingly, our studies have revealed that the conjugation of pTFT with cationic polymer positively affected the stability of the drug in aqueous solutions. It is known that TFT is readily hydrolyzed into 5-carboxy-2′-deoxyuridine by the attack of hydroxide ion on the undissociated or anionic species, with 5-hydroxydifluoromethyl-2′-deoxyuridine being the likely intermediate.[73] Therefore, while synthesizing the TFT−polymer conjugates, we were concerned with the possibility that the three fluorine atoms in TFT could be replaced by the hydroxyl groups, since the reaction was carried out in aqueous solution at pH > 9. Fortunately, the TFT moiety remained intact upon conjugation, as confirmed by ^{19}F-NMR spectroscopy. Indeed, the spectra of PEI-LA-pTFT and PEI-LA-UA-pTFT contained the same signals as were found in the spectrum of parent trifluorothymidine monophosphate (the presence of the peak at $\delta \sim 100$ ppm, D_2O).

In situ studies demonstrated that conjugation of pTFT with cationic polymer PEI enhanced the resistance of the drug to metabolism in comparison to the underivatized anticancer drug. This was shown using ^{19}F NMR spectroscopy which allows a precise and reproducible determination of the structure of all fluorine-containing substances including the previously unknown reaction products simultaneously without additional experimental procedures.[74] The final catabolite (free fluoride anion, F^-) was detected after 3 h of PEI-LA-UA-pTFT conjugate incubation in human plasma (Supporting Information, Figure S6). At the same time, the half-life of TFT in the plasma of cancer patients was reported to be 18 min.[37] Thus, the polymeric drug is degraded to the fluorine-containing catabolites more slowly than free TFT.

The TFT-containing PEI conjugates are prodrugs, that need to be hydrolyzed to produce active antimetabolite pTFT. Recently, stimulus-sensitive drug strategies have been suggested for the design of drug delivery systems.[75,76] Among these stimuli, changes in acidity are particularly useful for treating tumors, because tumor tissues have a relatively acidic extracellular environment (pH ∼ 6.8) compared to that of the surrounding normal tissues.[77−82] In addition, once the drug enters cells via endocytosis, it becomes exposed to more acidic conditions (pH 5−6) encountered in endosomes and lysosomes.[83,84] Due to the presence of a variety of protonable amines, PEI has a tremendous buffering capacity between pH 7.2 and 5.0.[38] The amino groups of the polymer can absorb protons brought into the endosome by ATPase pump, which causes osmotic swelling and, therefore, induces the rupture of the vesicle. For example, a PEI-based formulation of a phosphorylated nucleoside analogue 5′-triphosphate of 5-fluoroadenosine arabinoside, in which the drug was bound to the carrier due to ionic interactions between its triphosphate group and the protonated amino groups of the polymer, demonstrated an efficient intracellular release of active drug.[85] To improve the intracellular gene delivery via endocytosis, the attempts have been made to chemically modify the polycations by substituting them with imidazolyl or histidine groups.[40−42] It was demonstrated that the imidazolyl substitution of PEI improved the efficiency of nucleic acid delivery by 3- to 4-fold.[40] The PEI-based conjugates described here, PEI-LA-pTFT and PEI-LA-UA-pTFT, demonstrated the ability to be internalized by human breast carcinoma MCF-7 cells. The data on *in vitro* cellular uptake (Supporting Information, Figure S7) and cytotoxicity (Table 4) confirmed the delivery of the pTFT into cancer cells by the PEI-LA-UA-pTFT conjugate.

The pTFT residue is attached to the polymer via phosphamide bonds, which are relatively stable under physiological conditions, but are hydrolyzed in acidic solutions.[61] It is known that aliphatic monoamides of phosphate monoesters are much more stable at pH 5 than phosphorimidazolides.[61] The hydrolysis of the former types of compounds occurs only at pH ≤ 3. The presence of imidazolyl groups in the PEI-LA-UA conjugate allowed the attachment of pTFT to the polymer via acid-labile imidazolyl-phosphamide bonds. The exposure to slightly acidic conditions inside the cells is expected to facilitate the hydrolysis of PEI-LA-UA-pTFT and quick release of the incorporated anticancer drug.

In fact, the acid sensitivity of the PEI-LA-UA-pTFT molecules was demonstrated in test tubes using UV−vis (Supporting Information, Figure S5) and high-resolution ^{31}P NMR spectroscopy (Figure 8). PEI-LA-UA-pTFT was found to be acid-sensitive, while the control PEI-LA-pTFT was stable at pH 5.0 and 7.0. The data on the pTFT release from PEI-LA-UA-pTFT showed that 8.6% of the conjugate was hydrolyzed within 11 h of incubation at pH 7.0, while at pH 5.0 the percentage of hydrolysis reached 13.2% (Figure S4 in Supporting Information). Expectedly, the release of pTFT from PEI-LA-pTFT at pH 5.0 was negligible: only ∼0.1% of the conjugate was hydrolyzed within 72 h.

In order to detect how conjugation of the cationic polymer affects the cytotoxic properties of phosphorylated drug (pTFT), we have compared cytotoxicity of PEI-LA-pTFT conjugates with a various content of pTFT per PEI molecule. The survival of MCF-7 cells after the 72 h treatment with a solution of phosphorylated nucleoside analog pTFT (0.04 mM) was higher than 90%. With concentration and incubation time fixed at 0.8 μM and 72 h, respectively, the cytotoxicity of the PEI-LA-pTFT conjugates was lower for higher degrees of the polymer substitution with pTFT (Table 4). We used this relatively long incubation period since it is sufficient for internalization of the drug-containing conjugates necessary to compare cytotoxicities of free and PEI-conjugated pTFT. Even though the cellular uptake of the PEI-LA-pTFT conjugate was the same as the uptake of the PEI-LA-UA-pTFT conjugate (Figure S7 in Supporting Information), the cytotoxicity of the latter was higher (Table 4), likely because the conjugates that initially entered the cells by endocytosis were transferred to the lysosomes, where the acidic environment facilitated the hydrolysis of the conjugate and the release of pTFT. The newly generated pTFT may cross the lysosome membrane and reach cytoplasm by passive diffusion. Current study indicated the role of imidazolyl groups in internalization of the drug-containing PEI conjugates and release of the active drug from

dx.doi.org/10.1021/bc3006072 | *Bioconjugate Chem.* 2013, 24, 780−795

the conjugates. Further optimization of the content of urocanic acid in the PEI conjugates is required for the conjugates to demonstrate maximum efficiency for the targeted cells and minimum toxicity for normal cells.

Finally, the *in vivo* antitumor activity of the PEI-LA-UA-pTFT conjugate was evaluated in C57BL/6 mice with the model of Krebs-2 ascitic carcinoma. The Krebs-2 mouse ascitic carcinoma model was chosen because the Krebs-2 tumor cells grew aggressively in the syngeneic C57BL/6 mice, which allowed us to readily determine whether the delivery of pTFT to the cells by the acid-sensitive PEI-LA-UA-pTFT conjugate can improve its *in vivo* antitumor activity. To evaluate the *in vivo* antitumor activity of the PEI-LA-UA-pTFT conjugate, C57BL/6-tumor-bearing mice were treated with normal saline or PEI-LA-UA-pTFT solution. MRI analysis based on the combination of ^{1}H- and ^{19}F-images was carried out to generate a full picture of the sample after the drug's administration by intraperitoneal injections (Figure 11).

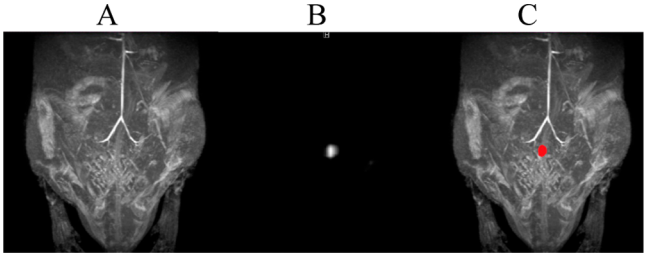

Figure 11. Reconstruction overlay of the ^{19}F and ^{1}H images revealing that ^{19}F signal emanates from peritoneum. The ^{19}F intensity is displayed on a "hot-iron" intensity scale, and the ^{1}H images are shown in gray scale. Shown (from left to right) are ^{1}H (A) and ^{19}F (B) images and a "composite" ^{19}F/^{1}H image (C).

Our initial results demonstrate the potential of PEI-LA-pTFT conjugates as MRS/MRI probes (Figures 9 and 11). However, more detailed studies with different TFT-containing PEI conjugates involving biodistribution (plasma clearance and organ distribution), toxicity, metabolic fate, and immunologic consequences are necessary to establish their potential as *in vivo* MRS/MRI probes.

As demonstrated in Table 5, the PEI-LA-UA-pTFT conjugate was effective in inhibiting the tumor growth. The enhanced antitumor activity may be attributed to the enhanced accumulation of PEI-LA-UA-pTFT inside the tumor, the lysosomal delivery of the conjugate, and faster acid-sensitive release of pTFT from the polymeric carrier in lysosomes. These results provide a strong basis for further investigation of PEI-LA-UA-pTFT conjugate as a promising tool for cancer therapy. In addition, when activated to its triphosphate form, TFT can be incorporated into a viral DNA and disrupt viral DNA synthesis. Furthermore, recent studies have reported strong inhibitor effect of PEI on human papillomaviruses, which are associated with anogenital malignancies and are etiologically linked to the development of cervical cancer.[86] PEIs and their derivatives may have a microbicide potential as prophylactic and therapeutic antiviral agents. Taken together, these results and our data indicate that PEI derivatives of TFT may be attractive for the development of antiviral microbicides and anticancer chemotherapy agents. Further studies aimed at testing the optimized PEI derivatives for their anticancer potential and investigating these conjugates for their antiviral efficiency in animal models are required.

EXPERIMENTAL PROCEDURES

Materials and Methods. **TFT** was purchased from U.S. Pharmacopeia (Rockville, MD). **PEI** (25 kDa) was purchased from Aldrich (USA): ^{13}C NMR (D_2O): δ 40.3 (m, $NH_2(CH_2)$), 48.6 (m, $NH(CH_2)_2$), 54.0 ppm (m, $N(CH_2)_3$).

All solvents and reagents, unless stated differently, were purchased from Sigma-Aldrich (St. Louis, MO) at the highest available grade and used without purification. Cascade Blue ethylenediamine trisodium salt and MTT (3-[4,5-dimethylthiazol-2-yl]-2,5-diphenyltetrazolium bromide) assay kit were purchased from Invitrogen. Plasma was separated from the freshly drawn human blood of 20 healthy volunteers without microvascular or macrovascular complications. The study was approved by the local ethic committee and performed in accordance with the International Conference on Harmonisation Guideline for Good Clinical Practice (1996), which represents the international ethical and scientific quality standard for designing, conducting, recording, and reporting trials that involve participation of human subjects. Solution of α-fetoprotein in water (AFP, 1 mg/mL) was purchased from "Vector-Best" (Novosibirsk, Russia) and additionally purified from fatty acids.

^{1}H and ^{19}F NMR spectra were recorded on AV-300 NMR spectrometer (Bruker, Rheinstetten, Germany) at 300 and 282 MHz, respectively. The spectra were detected at 25 °C in 5 mm NMR sample tubes. The chemical shifts were expressed in parts per million, ppm (δ). All ^{1}H chemical shifts were calculated relative to the residual ^{1}H NMR signal of the deuterated NMR solvent (D_2O, δ 4.80 ppm). C_6F_6 (δ 0.00 ppm) was used as an external reference for chemical shifts in ^{19}F NMR spectra. The ^{13}C NMR spectra were recorded on AV-400 NMR spectrometer (Bruker, Rheinstetten, Germany) at 100 MHz. ^{31}P NMR spectra were recorded on AV-400 and AV-300 NMR spectrometers (Bruker, Rheinstetten, Germany) at 162 and 121.5 MHz, respectively. The ^{31}P chemical shifts were reported using an external standard of 85% H_3PO_4. The spin−spin coupling constants (J) are reported in hertz (Hz) and spin multiples are given as s (singlet), d (doublet), t (triplet), q (quartet), m (multiplet), t.d (triplet of doublets), and br.s (broad singlet).

Electronic absorption spectra were acquired on a UV-1800 spectrometer (Shimadzu, Japan).

Fluorescence measurements were carried out in PBS (pH 7.4; 1.7 mM KH_2PO_4, 5.2 mM Na_2HPO_4, 150 mM NaCl) at room temperature on a Varian Cary Eclipse spectrofluorometer (Varian, USA) using a 1 cm quartz cell. A protein solution (1×10^{-6} M) was titrated with a ligand (concentration of the ligand varied from 1×10^{-6} to 1×10^{-5} M). Changes in fluorescence were measured using the excitation wavelength λ_{exc} = 295 nm (5 nm slit) and the emission wavelength λ_{em} = 340 nm (10 nm slit). Because a relatively small concentration of the protein was used, large slit widths were set to obtain a sufficiently strong signal from a single Trp residue. Experimental fluorescence data ($F_0/F(c)$) were plotted as a function of the ligand concentration (F_0 − fluorescence of the free protein, $F(c)$ − fluorescence of the protein upon the ligand binding at ligand concentration c). Association equilibrium constant (K_a) was determined using Stern−Volmer equation: $F_0/F = 1 + K_a c$.

Low molecular weight materials (M_r < 3000 Da) were removed from solutions of polymer conjugates by centrifugal filtration using Centricon concentrators (Amicon Centriprep YM30, Millipore, Bedford, MA).

dx.doi.org/10.1021/bc3006072 | *Bioconjugate Chem.* 2013, 24, 780−795

Synthesis of Trifluoromethyl-2′-deoxyuridine 5′-monophosphate (pTFT). pTFT was synthesized by Dr. Nina S. Kasatkina according to the published procedure[87] and purified by HPLC to an average purity of 99%. UV−vis (15 mM KH_2PO_4, pH 7.4):λ_{max} = 262 nm; $\varepsilon = 8.25 \times 10^3$ M^{-1} cm^{-1}. ^{31}P NMR (D_2O): δ 0.6 (s). ^1H NMR (D_2O): δ 2.28 (m, 2H, H-2′), 3.92 (m, 2H, H-5′), 4.08 (t.d, 1H, $J_{4'H\text{-}3'H}$ = 5.78, $J_{2'H\text{-}3'H}$ = 1.89, H-3′), 4.40 (t.d, 1H, $J_{3'H\text{-}4'H}$ = 5.78, $J_{5'H\text{-}4'H}$ = 2.82, H-4′), 6.11 (t, 1H, J = 6.7, H-1′), 8.29 (s, 1H, H-6). ^{19}F NMR (D_2O): δ 102.17 ppm.

Synthesis and Characterization of Linoleic Acid-Substituted Polyethyleneimine (PEI-LA, Figure S1 in Supporting Information). The synthetic procedure was adapted from Neamnark et al.[53] Detailed synthetic procedures and spectroscopic data of synthesized compound are given in Supporting Information.

Synthesis of Urocanic Acid-Substituted Polyethyleneimine via *N*-Hydroxysuccinimide Ester of Urocanic Acid (PEI-LA-UA, Figure 2). Urocanic acid (75.0 mg, 0.54 mmol) and *N*-hydroxysuccinimide (68.3 mg, 0.6 mmol) were dissolved in DMSO (1.2 mL). *N,N′*-Dicyclohexylcarbodiimide (DCC) (123.6 mg, 0.6 mmol) was dissolved in DMSO (0.8 mL). These solutions were mixed and were kept at 25 °C for 20 h. The reaction was monitored by TLC (thin layer chromatography) on silica, using a mixture of dichloromethane/ethanol (4:1 by vol) as eluent and visualized by UV. After the starting material was consumed, the *N,N′*-dicyclohexylurea was removed from solution by centrifugation and the *N*-hydroxysuccinimide ester of urocanic acid was used for the subsequent condensation without additional purification. The solution of PEI-LA (337.5 mg, 13.5 μmol) in DMSO (3.85 mL) was added to the solution of the *N*-hydroxysuccinimide ester of urocanic acid (40- to 100-fold excess of urocanic acid ester). The reaction mixture was incubated at 37 °C with stirring at 400 rpm. After 4 h, diethyl ether (10 mL) was added to the mixture to precipitate the polymeric product. The pellet was separated by centrifugation, washed with diethyl ether (10 mL × 3), and dissolved in 5 mL of DMSO. The resultant PEI-LA-UA conjugate was purified from low molecular weight compounds by centrifugal filtration using Centricon concentrators. The modified polymer was analyzed by ^1H NMR. The characteristic chemical shifts for the protons of UA (δ 6.48 ppm, H−f) and PEI (δ 2.4−3.6 ppm) were integrated, normalized for the number of protons in each peak, and used to evaluate the extent of urocanic substitutions on the modified polymer. At the *N*-hydroxysuccinimide ester of urocanic acid: PEI-LA molar ratios of 40, 60, and 100, the extent of urocanic acid substitutions were calculated to be 30, 40, and 80 urocanic acid residues per PEI molecule, respectively. The polymer conjugates containing 30 UA residues per PEI molecule were used in this study.

UV−vis (15 mM KH_2PO_4, pH 7.4): λ_{max} = 285 nm; $\varepsilon = 5.76 \times 10^5$ M^{-1} cm^{-1}. The characteristic proton shifts of the PEI-LA-UA-30 conjugate (Figure 3B) are: **PEI**: N−CH_2−CH_2−N, δ 2.4−3.6 (m, 2300 H). **LA**: δ 0.94 (m, 6H, H−d), 1.41 (m, 32H, H−b), 5.03 (m, H−e). **UA**: δ 6.48 (m, 30H, H−f), 7.45 (m, 60H, H−h,g), 7.87 ppm (m, 30H, H−i). ^{13}C NMR (D_2O): δ 32.6 (m, UA-NH(CH_2)), 37.8 (m, NH_2(CH_2)), 46.0 (m, NH(CH_2)$_2$), 51.3 (m, N(CH_2)$_3$), 117.3 (d, J = 161, C═C, C-f), 121.9 (d, J = 189, C═C, C-g), 132.0 (d, J = 159, C_{im}, C-h), 135.1 (s, C_{im}-C═C), 138.2 (d, J = 209, C_{im}, C-i), 169.2, 175.4, and 180.8 (s, C═O).

Synthesis of PEI-LA-UA-pTFT Conjugates. DMAP-pTFT (0.036 mmol) was reacted with PEI-LA-UA (0.9 μmol) in 0.26 mL of H_2O. The reaction mixture was stirred at 400 rpm at room temperature. After 1 h of reaction, low molecular weight reactants were removed from the polymeric product by centrifugal filtration using Centricon concentrators. The PEI-LA-UA:pTFT ratios were systematically varied during the synthesis procedure between 0.07 and 0.12 assuming one primary amine per PEI monomer unit. The polymer conjugates containing 40 pTFT residues per PEI molecule were used in this study. UV−vis (15 mM KH_2PO_4, pH 7.4): λ_{max} = 267 nm; $\varepsilon = 8.05 \times 10^5$ M^{-1} cm^{-1}.

The modified polymer was analyzed by ^1H NMR. The characteristic proton shifts of the PEI-LA-UA-pTFT-40 conjugate: **PEI**: N−CH_2−CH_2−N, δ 2.4−3.6 (m, 2300 H). **LA**: δ 0.9 (m, 6H, H−d); 1.4 (m, 32H, H−b), 1.5 (m, 4H, H−a). **UA**: δ 6.48 (m, 30H, H−f), 7.25 (m, 60H, H−h,g), 7.70 (m, 30H, H−i). **TFT**: δ 2.40 (m, 80H, H−m), 4.00 (m, 80H, H−j), 4.17 (m, 40H, H−l), 4.50 (m, 40H, H−k), 6.26 (m, 40H, H−n), 8.16 (m, 40H, H−o). ^{19}F NMR: −CF_3, δ 101.5 ppm (br.s). ^{31}P NMR: δ −10.87 (br.s, 1P), 8.83 (br.s, 1P).

Drug Release Properties of PEI-LA-pTFT-UA Conjugates at Different pH. Detailed kinetics of the hydrolysis of PEI conjugates based on the changes in absorption of the polymeric fraction are given in Supporting Information (Figure S5).

High-Resolution ^{31}P NMR Spectroscopy. PEI-LA-pTFT-UA in acetate buffer (1.5 mM, pH 5.0 or 7.0) at 0.1 M was incubated at 37 °C. At predetermined time points, the samples were analyzed by high-resolution ^{31}P NMR spectroscopy using an AV-300 NMR spectrometer.

Cell Culture. Tumor cell line from human mammary adenocarcinoma MCF-7 was grown in IMDM (Invitrogen) supplemented with 100 U/mL penicillin, 100 μg/mL streptomycin, and 10% fetal bovine serum (FBS) (Invitrogen) at 37 °C, 5% CO_2 in humid atmosphere.

***In Vitro* Cytotoxicity.** The inhibition of cell proliferation was determined using a colorimetric assay based on the cleavage of MTT (3-(4,5-dimethylthiazol-2-yl)-2,5-diphenyltetrazolium bromide) by mitochondrial dehydrogenases in viable cells, leading to formazan formation (MTT test[64]). Briefly, exponentially growing cells were plated in 96-well plates (~2000 cells per well) and were allowed to attach overnight (16 h) at 37 °C in IMDM (5% CO_2). The solutions of PEI, PEI-LA, PEI-LA-pTFT, or PEI-LA-pTFT-UA conjugates were applied in medium with PEI-equivalent concentrations ranging from 0.7 to 7000 nM. Cell viability was assessed at 72 h after the start of the treatments by MTT (Sigma-Aldrich). An aliquot (10 μL) of MTT solution (25 mg/mL in PBS) was added to each well and the plates were incubated at 37 °C for 3 h. The medium was removed and the dark blue crystals of formazan that had formed were dissolved in 100 μL of DMSO. The absorbance was measured in a microplate reader Multiscan^R EX (Thermo Electron Corporation) at 570 nm (peak) and 620 nm (bottom).

The concentration of polymer that caused 50% inhibition of cell growth was calculated. The results are expressed as mean ± standard deviation. Assays were performed in triplicate and the entire experiment was repeated three times.

MRI/MRS. All animal experiments described in this report were conducted in accordance with the policies of the Institutional Animal Care. All MRI/MRS experiments were performed on a horizontal 11.7 T magnet interfaced with a

dx.doi.org/10.1021/bc3006072 | *Bioconjugate Chem.* 2013, 24, 780−795

digital spectrometer (Bruker, BioSpec 117/16 USR, Germany) operating at the ^{1}H resonance frequency of 500 MHz. Before conducting the MRI and MRS experiments, each mouse was anesthetized by injecting anesthetic thiopental sodium. The animal was placed in the prone position on an animal bed which was then slid into the magnet bore. A respiratory pillow placed underneath the lower torso was used to monitor respiration (SA Instruments, Stony Brook, NY, USA).

^{31}P MRS (Figures 9 and 10). Approximately 20 min before acquiring data, 0.3 mL of a 0.33 mM solution (74.6 mg/kg) of PEI-LA-pTFT-40 conjugate was injected intramuscularly in the region between shoulders. ^{31}P MRS experiments were carried out using a $^{31}P/^{1}H$ surface coil operating at 202.4/500.3 MHz. The coil was positioned above the injection region. A single-pulse sequence with repetition time/echo time (TR/TE) = 100/3 ms, 2048 averages, total acquisition time 3.24 min was used for detecting ^{13}P NMR spectra *in vivo*. The spectral width was 40 ppm. This approach normally allows one to quantify the tissue content of five groups of metabolites exhibiting the total of seven NMR signals: phosphomonoesters (PME, 6 ppm), inorganic phosphate (P_i, 5 ppm), phosphodiesters (PDE, 2 ppm), phosphocreatine (PCr, 0 ppm), and adenosine triphosphate (ATP, −2.7, −7.8, −16.5 ppm). In our studies, an additional peak belonging to pTFT in the PEI-LA-pTFT conjugate was detectable at 12 ppm, *i.e.*, with a chemical shift significantly different from the ^{31}P NMR signals of five naturally occurring metabolites.

^{19}F MRI. Immediately before placing the animal in the magnet, 0.2 mL of a 0.063 mM solution of PEI-LA-UA-pTFT-40 conjugate (24 mg/kg) was injected intraperitoneally. Experiments were performed using the $^{19}F/^{1}H$ volume coil operating at 470.6/500.3 MHz. The ^{1}H image was obtained using a rapid acquisition with relaxation enhancement (RARE) fast spin−echo sequence with the following acquisition parameters: repetition time/echo time (TR/TE) = 2000/7.5 ms, RARE factor = 8, 256 × 256 matrix, field of view (FOV) = 60 × 60 mm^2, total acquisition time 1.36 min. For ^{19}F images, a RARE sequence was used with repetition time/echo time (TR/TE) = 1000/7.5 ms, RARE factor = 4, 128 × 64 matrix, field of view (FOV) = 60 × 60 mm^2, 32 averages, total acquisition time 6.24 min.

Animal Care and Maintenance of Tumors. Mice of C57Bl/6 strain were bred and kept under the standard vivarium conditions at the Institute of Cytology and Genetics, Siberian Branch of Russian Academy of Sciences. Mice were housed on a 12 h/12 h light/dark regimen. Animals were provided with food (pellet) and water *ad libitum*. Female C57Bl/6J mice, 10−12 weeks of age, were housed before the experiment in single litter groups of 4 individuals in 32 × 23 × 12 cm^3 cages. All experimental procedures were in compliance with the European Communities Council Directive of November 24, 1986 (86/1986/EEC).

Krebs-2 ascitic carcinoma was used in the experiments. The experimental mice received i.p. inocula of 10 mln tumor cells (day 0) obtained by removal of ascites fluid from tumor-bearing mice, centrifugation of the cells, and resuspension of the cells in appropriate (0.2 mL per mice) volume of saline. After tumor transplantation, the animals were divided into experimental and control groups and then were kept in their compartments until the end of the experiment. At the end of experiment the mice were decapitated and tumor-inhibitory activity was assessed. A T/C value (the ratio of the volumes of ascites in treated mice to that of control) was then computed, and this value was used to calculate the extent of tumor inhibition (1 − T/C × 100). The total numbers of tumor cells in treated and control mice were compared similarly as well.

***In Vivo* Antitumor Activity.** To evaluate the *in vivo* antitumor activity of the PEI-LA-UA-pTFT-40 conjugate, C57BL/6 female mice with ascites form of Krebs-2 tumor were treated with conjugate solution. The drug was administered by i.p. injections three times at a single dose of 24 mg/kg on days 2, 4, and 6 after tumor transplantation. Control animals received three corresponding injections of normal saline. The mice were weighed daily, and on day 8 they were decapitated, ascites was removed and weighed, the number of cells of the Krebs ascites carcinoma were counted, and the tumor-inhibitory activity was assessed. The ratio of the volumes of ascites in treated (T) to that of control (C) mice was 0.177, and the corresponding ratio for the tumor cell numbers was 0.012, indicating tumor growth inhibition of 82.3% and 98.9%, respectively.

The second experiment was performed to evaluate the effect of PEI-LA-UA-pTFT-40 conjugate on the life span of tumor-bearing mice. After treatment of animals as in the previous experiment, the mice were allowed to naturally die from tumors. While control mice survived for 8.9 ± 0.11 days after tumor transplantation, the treated ones lived more than 3 times longer (30.3 ± 3.12; $p < 0.001$) as compared to the control.

■ ASSOCIATED CONTENT

Ⓢ Supporting Information

Details on the synthesis of linoleic acid-substituted polyethyleneimine (PEI-LA), urocanic acid-substituted polyethyleneimine via pentafluorophenyl ester of urocanic acid (PEI-LA-UA), ligand-directed amidophosphate 5-trifluoromethyl-2′-deoxyturidine (PEI-LA-pTFT), phosphorylating derivative of 5-trifluoromethyl-2′-deoxyturidine 5′-monophosphate (DMAP-pTFT), and spectroscopic data for all synthesized compounds; detailed synthetic procedures of FITC-labeled PEI-LA-pTFT and PEI-LA-UA-pTFT and fluorescence micrographs of MCF-7 cells incubated with FITC-labeled PEI-based conjugates; kinetics of the hydrolysis of PEI conjugates based on the changes in absorption of the polymeric fraction; stability of the PEI-LA-UA-pTFT conjugate in human plasma. This material is available free of charge via the Internet at http://pubs.acs.org.

■ AUTHOR INFORMATION

Corresponding Author

*E-mail addresses: godov@niboch.nsc.ru and silnik@niboch.nsc.ru.

Notes

The authors declare no competing financial interest.

■ ACKNOWLEDGMENTS

We wish to thank Ms. V. V. Kandaurova (Novosibirsk Institute of Organic Chemistry, SB RAS) for technical assistance. The work was supported by Integration grant #60 from the SB RAS and by the RFBR grant #12-04-01454-a and partially supported by the program of the Russian Government to support leading scientists (11.G34.31.0045), and President Grant (NS-64.2012.4).

■ ABBREVIATIONS

SB RAS, Siberian Branch of the Russian Academy of Sciences

REFERENCES

(1) Patra, H. K., Banerjee, S., Chaudhuri, U., Lahiri, P., and Dasgupta, A. K. (2007) Cell selective response to gold nanoparticles. *Nanomedicine 3*, 111−119.

(2) McCarthy, J. R. (2009) The future of theranostic nanoagents. *Nanomedicine 4*, 693−695.

(3) Carbal, H., Nishiyama, N., and Kataoka, K. (2011) Supramolecular nanodevices: from design validation to theranostic nanomedicine. *Acc. Chem. Res. 44*, 999−1008.

(4) Carbal, H., and Kataoka, K. (2010) Multifunctional nanoassemblies of block copolymers for future cancer therapy. *Sci. Technol. Adv. Mater. 11*, 1−9.

(5) Zhao, Q., Wang, L., Cheng, R., Mao, L., Arnold, R. D., Howerth, E. W., Chen, Z. G., and Platt, S. (2012) Magnetic nanoparticle-based hyperthermia for head&neck cancer in mouse models. *Theranostics 2*, 113−121.

(6) Pan, D., Caruthers, S. D., Hu, G., Senpan, A., Scott, M. J., Gaffney, P. J., Wickline, S. A., and Lanza, G. M. (2008) Ligand-directed nanobialys as theranostic agent for drug delivery and manganese-based magnetic resonance imaging of vascular targets. *J. Am. Chem. Soc. 130*, 9186−9187.

(7) Lee, S.-M., Song, Y., Hong, B. J., MacRenars, K. W., Mastarone, D. J., O'Halloran, T. V., Meade, T. J., and Nguyen, S. T. (2010) Modular polymer-caged as a theranostic platform with enhanced magnetic resonance relaxivity and pH-responsive drug. *Angew. Chem., Int. Ed. 49*, 9960−9964.

(8) Carr, D. H., Brown, J., Bydder, G. M., Steiner, R. E., Weinmann, H. J., Speck, U., and Young, I. R. (1984) Gadolinium-DTPA as a contrast agent in MRI: initial clinical experience in 20 patients. *Am. J. Roentgenol. 143*, 215−224.

(9) Schmiedl, U., Ogan, M., Paajanen, H., Marotti, M., Crooks, L. E., Brito, A. C., and Brasch, R. C. (1987) Albumin labeled with Gd-DTPA as an intravascular, blood pool-enhancing agent for MR imaging: biodistribution and imaging studies. *Radiology 162*, 205−210.

(10) Caruthers, S. D., Wickline, S. A., and Lanza, G. M. (2007) Nanotechnological applications in medicine. *Curr. Opin. Biotechnol. 18*, 26−30.

(11) Abded-Kader, K., Patel, P. R., Kallen, A. J., Sinkowitz-Cochran, R. L., Bolton, W. R., and Unruh, M. L. (2010) Nephrogenic systemic fibrosis: a survey of nephrologists' perceptions and practice. *Clin. J. Am. Soc. Nephrol. 5*, 964−971.

(12) Ruiz-Cabello, J., Barnett, Barnett, B. P., Bottomley, P. A., and Butle, J. W. M. (2011) Fluorine (^{19}F) MRS and MRI in biomedicine. *NMR Biomed. 24*, 114−129.

(13) Gametti, M., Crousse, B., Metrangolo, M., Milani, R., and Resnati, G. (2012) The fluorous effect in biomolecular applications. *Chem. Soc. Rev. 41*, 31−42.

(14) Jiang, Z.-X., Liu, X., Jeong, E.-K., and Yu, Y. B. (2009) Symmetry-Guided Design and fluorous synthesis of a stable and rapidly excreted imaging tracer for ^{19}F MRI. *Angew. Chem., Int. Ed 48*, 4755−4758.

(15) Yu, J.-X., Kodibagkar, V. D., Cui, W., and Mason, R. P. (2005) ^{19}F: a versatile reporter for non-invasive physiology and pharmacology using magnetic resonance. *Curr. Med. Chem. 12*, 819−848.

(16) Lauterbur, P. C. (1973) Image formation by induced local interactions: examples employing nuclear magnetic resonance. *Nature 242*, 190−191.

(17) Holland, G. N., Bottomley, P. A., and Hinshaw, W. S. J. (1977) ^{19}F magnetic resonance imaging. *Magn. Reson. 28*, 133−136.

(18) Mason, R. P., Antich, P. P., Babcock, E. E., Gerberich, J. L., and Nunnally, R. L. (1989) Perfluorocarbon imaging in vivo: a ^{19}F MRI study of tumor bearing mice. *Magn. Reson. Imaging 7*, 474−485.

(19) Morawski, A. M., Winter, P. M., Yu, X., Fuhrhop, R. W., Scott, M. J., Hockett, F., Robertson, J. D., Gaffney, P. J., Lanza, G. M., and Wickline, S. A. (2004) Quantitative "magnetic resonance immunohistochemistry" with ligand-targeted ^{19}F nanoparticle. *Magn. Reson. Med. 52*, 1255−1262.

(20) Neubauer, A. M., Myerso, J., Caruthers, S. D., Hocket, F. D., Winter, P. M., Chen, J., Gaffney, P. J., Robertson, J. D., Lanza, G. M., and Wickline, S. A. (2008) Gadolinium-modulated ^{19}F signals from perfluorocarbon nanoparticles as a new strategy for molecular imaging. *Magn. Reson. Med. 60*, 1066−1072.

(21) Kimura, A., Narazaki, M., Kanazawa, Y., and Fujiwara, H. (2004) ^{19}F magnetic resonance imaging of perfluorooctanoic acid encapsulated in liposome for biodistribution measurement. *Magn. Reson. Imaging 22*, 855−860.

(22) Nosé, Y. (2004) Is there a role for blood substitutes in civilian medicine: a drug emergency shock cases? *Artif. Organ. 28*, 807−812.

(23) Meyer, K. L., Carvlin, M. J., Mukherji, B., Slviter, H. A., and Joseph, P. M. (1992) Fluorinated blood substitute retention in the rat measured by fluorine-19 magnetic resonance imaging. *Invest. Radiol. 27*, 620−627.

(24) Plunkett, W., Huang, P., and Gandhi, V. (1995) Preclinical characteristics of gemcitabine. *Anti-Cancer Drugs 6*, 7−13.

(25) Noble, S., and Goa, K. L. (1997) Gemcitabine: A review of its pharmacology and clinical potential in non-small cell lung cancer and pancreatic cancer. *Drugs 54*, 447−472.

(26) Zhang, J., Visser, F., King, K., Baldwin, S., Young, J., and Cass, C. (2007) The role of nucleoside transporters in caner chemotherapy with nucleoside drugs. *Cancer Metastasis Rev. 26*, 85−110.

(27) Reid, J. M., Qu, W., Safgren, S. L., Ames, M. M., Krailo, M. D., Seibel, N. L., Kuttesch, J., and Holcenberg, J. (2004) Phase I trial and pharmacokinetics of gemcitabine in children with advanced solid tumors. *J. Clin. Oncol. 22*, 2445−2451.

(28) Reddy, L., H., Khoury, H., Paci, A., Deroussent, A., Ferreira, H., Dubernet, C., Declèves, X., Besnard, M., Chacum, H., Lepêtre-Mouelhi, S., Desmaële, D., Rousseau, B., Laugier, C., Cintrat, J.-C., Vassal, G., and Couvreur, P. (2008) Squalenoylation favorably modifies the in vivo pharmacokinetics and biodistribution of gemcitabine in mice. *Drug Metab. Dispos. 36*, 1570−1577.

(29) Ansfield, F. J., Ramirez, G., Mackman, S., Bryan, G. T., and Curreri, A. R. (1969) A ten-year study of 5-flurouracil I disseminated breast cancer with clinical. *Cancer. Res. 29*, 1062−1066.

(30) Pinedo, H. M., and Peters, G. J. (1988) Fluorouracil: biochemistry and pharmacology. *J. Clin. Oncol. 6*, 1653−1664.

(31) Presant, C. A., Multhauf, P., Klein, L., Chan, C., Chang, F. F., Hum, G., Joseph, R., Lemkin, S., Shiftan, T., and Plotkin, D. (1983) Thymidine and 5-FU: Phase II pilot study in colorectal and breast carcinomas. *Cancer Treat. Rep. 67*, 735−736.

(32) Peters, G. J., Backus, H. H., Freemantle, S., van Triest, B., Codacci-Pisanelli, G., van der Wilt, C. L., Smid, K., Lunec, J., Calvert, A. H., Marsh, S., McLeod, H. L., Bloemena, E., Meijer, S., Jansen, G., van Groeningen, C. J., and Pinedo, H. M. (2002) Induction of thymidylate synthase as a 5-fluorouracil resistance mechanism. *Biochim. Biophys. Acta 1587*, 194−205.

(33) Temmink, O. H., Emura, T., de Bruin, M., Fukushima, M., and Peters, G. J. (2007) Therapeutic potential of the dual-targeted TAS-102 formulation in the treatment of gastrointestinal malignancies. *Cancer Sci. 98*, 779−789.

(34) Overman, M. J., Kopetz, S., Varadhachary, G., Fukushima, M., Kuwata, K., Mita, A., Wolff, R. A., Hoff, P., Xiong, H., and Abbruzzese, J. L. (2008) Phase I clinical study of three times a day oral administration of TAS-102 in patients with solid tumors. *Cancer Invest. 26*, 794−799.

(35) Heidelberger, C., and Anderson, S. W. (1964) Fluorinated pyrimidines. XXI. The tumor inhibitory activity of 5-trifluoromethyl-2′-deoxyuridine. *Cancer Res. 24*, 1979−1985.

(36) Bijnsdorp, I. V., Peters, G. J., Temmink, O. H., Fukushima, M., and Kruyt, F. A. (2010) Differential activation of cell death and autophagy results in an increased cytotoxic potential for trifluorothymidine compared to 5-fluorouracil in colon cancer cells. *Int. J. Cancer 126*, 2457−2468.

(37) Dexter, D. L., Wolberg, W. H., Ansfield, F. J., Helson, L., and Heidelberger, C. (1972) The clinical pharmacology of 5-trifluoromethyl-2′-deoxyuridine. *Cancer Res. 32*, 247−253.

(38) Mintzer, M. A., and Simanek, E. E. (2009) Nonviral vectors for gene delivery. *Chem. Rev. 109*, 259−302.
(39) Thomas, M., and Klibanov, A. M. (2002) Enhancing polyethylenimine's delivery of plasmid DNA into mammalian cell. *Proc. Natl. Acad. Sci. U.S.A. 99*, 14640−14645.
(40) Swami, A., Aggarwal, A., Patnaik, S., Kumar, P., Singh, Y., and Gupta, K. C. (2007) Imidazolyl-PEI modified nanoparticles for enhanced gene delivery. *Pharm. Nanotechnol. 335*, 180−192.
(41) Kim, T. H., Ihm, J. E., Choi, Y. J., Nah, J. W., and Cho, C. S. (2003) Efficient gene delivery by urocanic acid-modified chitosan. *J. Controlled Release 93*, 389−402.
(42) Jin, H., Kim, T. H., Hwang, S.-K., Chang, S.-H., Kim, H. W., Anderson, H. K., Lee, H.-W., Lee, K.-H., Colburn, N. H., Yang, H.-S., Cho, M.-H., and Cho, C S. (2006) Aerosol delivery of urocanic acid-modified chitosan/programmed cell death 4 complex regulated apoptosis, cell cycle, and angiogenesis in lungs of K-*ras* null mice. *Mol. Cancer Ther. 5*, 1041−1049.
(43) Deutsch, H. F. (1991) Chemistry and biology of alpha-fetoprotein. *Adv. Cancer Res. 56*, 253−312.
(44) Mizejewski, G. J. (2011) Review of the putative cell-surface receptors for alpha-fetoprotein: identification of a candidate receptor protein family. *Tumor Biol. 2*, 241−258.
(45) Sorentino, D., Stump, D., Potter, B. J., Robinson, R. B., White, R., Kiang, C., and Berk, P. D. (1988) Oleate uptake by cardiac myocytes is carrier mediated and involves a 40-kD plasma membrane fatty acid binding protein similar that in liver, adipose tissue, and gut. *J. Clin. Invest. 82*, 928−935.
(46) Uriel, J., Naval, J., and Laborda, J. (1987) AFP-mediated transfer of arachidonic acid into cultured cloned cells derived from a rat rhabdhomyosacoma. *J. Biol. Chem. 262*, 3579−3585.
(47) Uriel, J., Laborda, J., Naval, J., Geuskens, M. (1989) Alpha-fetoprotein receptors is malignant cells. An overview. In *Biologica Activities of AFP* (Mizejewski, G. J., and Jacobson, H. I., Ed.) pp 103−117, Vol. *II*, CRC Press, Boca Raton.
(48) Torres, J. M., Laborda, J., Naval, J., Darracq, N., Mishal, Z., and Uriel, J. (1989) Expression of alpha-fetoprotein receptors by human T-lymphocytes during blastic transformation. *Mol. Immunol. 26*, 851−857.
(49) Esteban, Ch., Geuskens, M., and Uriel, J. (1991) Activation of an alpha-fetoprotein (AFP)/receptor autocrine loop in HT-29 human colon carcinoma cell. *Int. J. Cancer 49*, 425−430.
(50) Klotz, I. M., and Sloniewsky, A. R. (1968) Macromolecule-small molecule interactions: a synthetic polymer with greater affinity than serum albumin for small molecules. *Biochem. Biophys. Res. Commun. 31*, 421−426.
(51) von Harpe, A., Petersen, H., Li, Y., and Kissel, T. (2000) Characterization of commercially available and synthesized polyethylenimines for gene delivery. *J. Controlled Release 69*, 309−322.
(52) Aravindan, L., Bicknell, K. A., Brooks, G., Khutoryanskiy, V. V., and Williams, A. C. (2009) Effect of acyl chain length on transfection efficiency and toxicity of polyethylenimine. *Int. J. Pharm. 378*, 201−210.
(53) Neamnark, A., Suwantong, O., Bahadur, R., Hsu, C. Y. M., Supaphol, P., and Uludag, H. (2009) Aliphatic lipid substitution on 2 kDa polyethylenimine improves plasmid delivery and transgene expression. *Mol. Pharmaceutics 6*, 1798−1815.
(54) von der Vusse, G. J. (2009) Albumin as fatty acid transporter. *Drug Metab. Pharmacokinet. 24*, 300−307.
(55) Iturralde, M., Alava, M. A., González, B., Anel, A., and Piñeiro, A. (1991) Effect of α-fetoprotein and albumin on the uptake of polyunsaturated fatty acids by rat hepatoma cells and fetal rat hepatocyte. *Biochim. Biophys. Acta 1086*, 81−88.
(56) Kinuta, M., Masuoka, N., Ohta, J., Teraoka, T., and Ubuka, T. (1991) Isolation and characterization of 3-[(carboxymethyl)]-3-(1H-imidazol-4-yl)propanoic acid from humn urine and preparation of its proposed precursor, S-[2-carboxy-1-(1H-imidazol-4-yl)ethyl]-cysteine. *Biochem. J. 275*, 617−621.
(57) Neuvonen, H., and Neuvonen, K. (1998) Investigation of the applicability of cis-urocanic acid as a model for the catalytic Asp-His dyad in the active site of serine proteases based on ^{1}H NMR hydrogen bonding studies and spectroscopic pK_a measurements. *J. Chem. Soc., Perkin Trans. 2*, 1665−1670.
(58) Mehler, A. H., and Tabor, H. (1952) Deamination of histidine to form urocanic acid in liver. *Federation Proc. 11*, 775−784.
(59) Godovikova, T. S., Zarytova, V. F., and Khalimskaya, L. M. (1986) Reactive phosphamidates of mono- and dinucleotides. *Sov. J. Bioorg. Chem. 12*, 475−481.
(60) Lebedev, A. V., and Rezvukin, A. I. (1984) Tendencies of ^{31}P chemical shifts changes in NMR spectra of nucleotide derivatives. *Nucleic Acids Res. 12*, 5547−5566.
(61) Godovikova, T. S., Grachev, M. A., Kutyavin, I. V., Tsarev, I. G., Zarytova, V. F., and Zaychikov, E. F. (1987) Studies of the functional topography of Escherichia coly RNA polymerase. Affinity labeling of RNA polymerase in a promoter complex by phosphorylating derivatives of primer oligonucleotides. *Eur. J. Biochem. 166*, 611−616.
(62) McSheehy, P. M. J., Seymour, M. T., Ojugo, A. S. E., Rodrigues, L. M., Leach, M. O., Judson, I. R., and Griffiths, J. R. (1997) A pharmacokinetic and pharmacodynamic study in vivo of human HT29 tumours using ^{19}F and ^{31}P magnetic resonance spectroscopy. *Eur. J. Cancer 33*, 2418−2427.
(63) Villacampa, M. J., Moro, R., Naval, J., Failly-Crepin, C., Lampreave, F., and Uriel, J. (1984) Alpha-fetoprotein receptors in a human breast cancer cell line. *Biochem. Biophys. Res. Commun. 122*, 1322−1327.
(64) Mosmann, T. (1983) Rapid colorimetric assay for cellular growth and survival − application to proliferation and cyto-toxicity assays. *J. Immunol. Methods 65*, 55−63.
(65) Choksakulnimitr, S., Masuda, S., Tokuda, H., Takakura, Y., and Hashida, M. (1995) In vitro cytotoxicity of macromolecules in different cell-culture systems. *J. Controlled Release 34*, 233−241.
(66) Morgan, D. M. L., Larvin, V. L., and Pearson, J. D. (1989) Biochemical-characterization of polycation-induced cyto-toxicity to human vascular endothelial cells. *J. Cell Sci. 94*, 553−559.
(67) Fischer, D., Li, Y. X., Ahlemeyer, B., Krieglstein, J., and Kissel, T. (2003) In vitro cytotoxicity testing of polycations: influence of polymer structure on cell viability and hemolysis. *Biomaterials 24*, 1121−1131.
(68) Lv, H. T., Zhang, S. B., Wang, B., Cui, S. H., Yan, J. (2006) Toxicity of cationic lipids and cationic polymers in gene delivery. *J. Controlled Release 114*, 100−109.
(69) Galmarini, C. M., Mackey, J. R., and Dumontet, C. (2002) Nucleoside analogues and nucleobases in cancer treatment. *Lancet Oncol. 3*, 415−424.
(70) Anslfield, F. J., and Ramirez, G. (1971) Phase I and II studies of 2′-deoxy-5-(trifluoromethyl)-uridine (NSC-75520). *Cancer Chemother. Rep. 55*, 205−208.
(71) Overman, M. J., Kopetz, S., Varadhachary, G., Fukushima, M., Kuwata, K., Mita, A., Wolff, R. A., Hoff, P., Xiong, H., and Abbruzzese, J. L. (2008) Phase I clinical study of three times a day oral administration of TAS-102 in patients with solid tumors. *Cancer Invest. 26*, 794−799.
(72) Feldman, N. F., Kiselev, S. M., Gukasova, N. V., Posypanova, G. A., Lutsenko, S. V., and Severin, S. E. (2000) Antitumor activity of α-fetoprotein conjugate with doxorubicin in vitro and in vivo. *Biochemistry 65*, 967−971.
(73) Nestler, H. J., and Garrett, E. R. (1968) Prediction of stability in pharmaceutical preparations. XV. Kinetics of hydrolysis of 5-trifluoromethyl-2-deoxyuridine. *J. Phar. Sci. 57*, 1117−1124.
(74) Malet-Martino, M., Gilard, V., and Desmoulin Martino, R. (2006) Fluorine nuclear magnetic resonance spectroscopy of human biofluids in the field of metabolic studies of anticancer and antifungal fluoropyrimidine drugs. *Clin. Chim. Acta 366*, 61−73.
(75) Kohli, E., Han, H.-Y., Zeman, A. D., and Vinogradov, S. V. (2007) Formulations of biodegradable Nanogel carriers with 5′-triphosphtes of nucleoside analogs that display a reduced cytotoxicity and enhanced drug activity. *J. Controlled Release 121*, 19−27.
(76) Zhu, S., Lansahara-P, D. S. P., Li, X., and Cui, Z. (2012) Lysosma delivery of a lipophilic gemcitabine prodru using novel acid-

sensitive micelles improved its antitumor activity. *Bioconjugate Chem. 23*, 966−980.
(77) Newell, K., Franchi, A., Pouyssegur, J., and Tannock, I. (1993) Studies with glycolysis-deficient cells suggest that production of lactic acid is not the only cause of tumor acidity. *Proc. Natl. Acad. Sci. U.S.A. 80*, 1127−1131.
(78) Yamagata, M., Hasuda, K., Stamato, T., and Tannock, I. F. (1998) The contribution of lactic acid to acidification of tumours: studies of variant cells lacking lactate dehydrogenase. *Br. J. Cancer 77*, 1726−1731.
(79) Stubbs, M., McSheehy, P. M. J., and Griffiths, J. R. (1999) Causes and consequences of acid pH in tumours: a magnetic resonance study. *Adv. Edv. Enzyme Regul. 39*, 13−30.
(80) Stubbs, M., Rodrigues, L. M., Howe, F. A., Wang, J., Jeong, K. S., Veech, R. L., and Griffiths, J. R. (1994) The metabolic consequences of a reversed pH gradient in rat tumours. *Cancer Res. 54*, 4011−4016.
(81) Gerweck, L. E., and Seetharaman, K. (1996) Cellular pH gradient in tumor versus normal tissue: potential exploitation for the treatment of cancer. *Cancer Res. 56*, 1194−1198.
(82) Ojugo, A. S. E., McSheehy, P. M. J., Stubbs, M., Alder, G., Bashford, C. L., Maxwell, R. J., Leach, M. O., Judson, I. R., and Griffiths, J. R. (1998) Influence of pH on the uptake of 5-fluorouracil into isolated tumor cells. *Br. J. Cancer 77*, 873−879.
(83) Haag, R. (2004) Supramolecular drug-delivery systems based on polymeric core-shell architectures. *Angew. Chem., Int. Ed. Engl. 43*, 278−282.
(84) Engin, K., Leeper, D. B., Cater, J. R., Thistlethwaite, A. J., Tupchong, L., and McFarlane, J. D. (1995) Extracellular pH distribution in human tumours. *Int. J. Hyperthermia 11*, 211−216.
(85) Vinogradov, S. V., Zeman, A. D., Batrakova, E. V., and Kabanov, A. V. (2005) Polyplex nanogel formulations for drug delivery of cytotoxic nucleside analogs. *J. Controlled Release 107*, 143−157.
(86) Spoden, G. A., Besold, K., Krauter, S., Plachter, B., Hanik, N., Kilbinger, A. F. M., Lambert, C., and Florin, L. (2012) Polyethylenimine is a strong inhibitor of human papillomavirus and cytomegalovirus infection. *Antimicrob. Agents Chemother. 56*, 75−82.
(87) Ludwig, J. (1981) A new route to nucleoside-5′triphosphates. *Acta Biochim. Biophys. Acad. Sci. Hung. 16*, 131−133.